Computer Modeling in Engineering & Sciences

Tech Science Press

https://doi.org/10.32604/cmes.2026.082535

REVIEW

Review on Phase-Field Modeling of Fracture in Ferroelectric Materials

Shuai Wang[1,*], **Ke Han**[1] **and Min Yi**[2,*]

[1]Hangzhou International Innovation Institute of Beihang University, Hangzhou, China
[2]State Key Laboratory of Mechanics and Control for Aerospace Structures & Institute for Frontier Science & College of Aerospace Engineering, Nanjing University of Aeronautics and Astronautics (NUAA), Nanjing, China

*Corresponding Authors: Shuai Wang. Email: swang@buaa.edu.cn; Min Yi. Email: minyi@nuaa.edu.cn

Received: 17 March 2026; Accepted: 12 May 2026; Published: 30 June 2026

ABSTRACT: Ferroelectric materials, integral to modern sensors, actuators, and transducers, exhibit complex fracture behavior under coupled electromechanical loading due to the intrinsic interplay between cracks, domain structures, and microstructural features. Linear piezoelectric fracture mechanics provides a foundational framework but fails to capture nonlinearities induced by domain switching and microstructure. This review synthesizes advances in computational modeling of ferroelectric fracture, with a focus on the unifying capabilities of the phase-field method (PFM). We first establish the fundamentals, including fracture toughness anisotropy and the crack-tip flexoelectric effect. We then critically assess traditional approaches like cohesive zone models and the extended finite element method, highlighting their limitations in handling arbitrary crack paths and complex microstructure evolution. The core of the review details how PFM has emerged as a transformative paradigm, enabling the simulation of diffuse crack propagation seamlessly coupled with ferroelectric domain dynamics within a single variational framework. We systematically examine recent progress in applying this framework to model fracture coupled with explicit microstructure (e.g., grains and domain walls), dielectric breakdown, fatigue under cyclic loading, and the integration of machine learning for model acceleration and inverse design. The review concludes by identifying persistent challenges, such as reconciling crack-face boundary conditions and bridging atomic-scale mechanisms with polycrystal-scale failure, and outlines future research directions toward predictive, multiscale, and experimentally validated models for designing reliable next-generation ferroelectric devices.

KEYWORDS: Fracture; ferroelectrics; phase field; material modeling; ceramics; piezoelectrics

1 Introduction

Since the discovery of ferroelectric oxides in the 1940s, their unique electromechanical properties have motivated theoretical developments in ferroelectricity and practical efforts to manufacture inexpensive yet reliable electronic devices, including sensors, actuators, and transducers [1]. Industrial-use ferroelectric oxides appear in various forms: ceramics, single crystals, and thin films. Ferroelectric ceramics typically exhibit brittle behavior under high electric fields and mechanical loading. Traditional ferroelectric ceramics undergo electric break down when subjected to a critical electric field (normally $2\,\mathrm{kV\,mm^{-1}}$) or crack under a critical mechanical load (normally 100 MPa). Their fracture toughness remains low (around $1\,\mathrm{MPa}\sqrt{\mathrm{m}}$), Domain structure distinguishes ferroelectrics from other materials and underlies their nonlinear macroscopic response. Given the inherent characteristics of ferroelectric polycrystals—electromechanical coupling, polarization heterogeneity, and complex microstructure—experimental and theoretical fracture mechanics investigations must incorporate electric field effects, domain configurations,

and grain-level information. The inherent brittleness of ferroelectric ceramics demands rigorous understanding of fracture mechanisms under coupled electromechanical loading. Linear piezoelectric fracture mechanics (LPFM) extends classical fracture theory by introducing electric displacement intensity factors (EDIF) and energy release rates (ERR), providing an initial framework for analyzing crack-tip singularities in these materials [2,3]. However, LPFM exhibits significant limitations in predicting experimental observations, particularly concerning electric fields effects. Applied electric fields may either enhance or suppress fracture toughness depending on their polarity and orientation relative to the crack plane due to the nonlinear domain switching near crack tip [4,5]. This switching, particularly 90° reorientation, dissipates energy through localized ferroelastic deformation, effectively shielding the crack tip. Conversely, electrical boundary conditions at crack surfaces remain contentious: impermeable crack assumptions (zero dielectric permittivity) overestimate field shielding, while permeable models neglect the dielectric properties of crack-filling media. Semi-permeable models (e.g., PKHS model) [6,7] partially address this issue but still struggle to capture dynamic crack-defect interactions, such as oxygen vacancy and pinning of domain walls under cyclic loading. These unresolved complexities underscore the need for advanced theoretical frameworks that integrate microscale domain dynamics with macroscale fracture criteria—a challenge further complicated by the history-dependent nature of ferroelectric hysteresis.

The fracture behavior of ferroelectric materials is intrinsically governed by their complex microstructure. Experimental studies reveal that grain size critically influences crack propagation paths: coarse-grained ceramics exhibit predominantly transgranular cracking, while fine-grained counterparts favor intergranular fracture, leading to up to twofold differences in fracture toughness [8,9]. Domain switching, particularly 90° reorientation near crack tips, locally dissipates energy to enhance fracture resistance by impeding crack growth [10]. Conversely, defects such as oxygen vacancies accelerate fatigue by pinning domain walls and promoting crack initiation under cyclic loading [11]. These microstructural interactions between grains, domains, and defects collectively dictate macroscopic fracture responses. However, experimental approaches face challenges in decoupling interdependent variables (e.g., isolating grain-size effects from boundary contributions) and in capturing dynamic crack-microstructure interactions. This limitation underscores the need for computational tools that bridge microstructural complexity and fracture mechanics.

Simulation of fracture in ferroelectric materials has evolved considerably to address LPFM limitations, particularly its inability to fully capture electromechanical coupling and microstructure-dependent nonlinearities. Early cohesive zone models (CZM) and extended finite element methods (XFEM) encountered difficulties resolving dynamic interactions among cracks, domain switching, and defects. Phase-field modeling (PFM) emerged as an alternative by treating cracks and domain walls as diffuse interfaces, enabling explicit simulation of microstructure evolution (e.g., grain boundaries, 90° domain switching) and their influence on fracture toughening or weakening. Recent advances incorporate flexoelectric effects, dielectric breakdown, and fatigue mechanisms, while machine learning (ML) extensions facilitate parametric studies of microstructural variables. Nevertheless, key challenges persist: reconciling electrical boundary conditions at crack faces (impermeable vs. permeable assumptions), quantifying defect-domain interactions (e.g., oxygen vacancy pinning) under cyclic loading, and bridging atomic-scale switching dynamics with polycrystal-scale crack propagation. These unresolved issues underscore the need for multiscale, experimentally validated phase-field frameworks to achieve predictive fracture models for next-generation ferroelectrics.

This article reviews current understanding of fracture mechanics in ferroelectric materials, emphasizing simulation methodologies that connect microscale domain dynamics with macroscale crack propagation. Section 2 establishes the fundamentals of ferroelectric fracture, covering LPFM, fracture toughness anisotropy, and crack-tip flexoelectric effects. Section 3 critically evaluates traditional modeling approaches,

including CZM, XFEM and PFM for fracture, highlighting their limitations in capturing electromechanical coupling and microstructure evolution. Section 4 examines phase-field modeling for ferroelectricity, emphasizing its capability to simulate polarization switching, domain wall motion, and grain-boundary interactions. Section 5 synthesizes advances in phase-field modeling of ferroelectric fracture, integrating microstructure (grains, domains, defects), flexoelectric effects, dielectric breakdown, fatigue mechanisms, and ML extensions. This review prioritizes studies addressing multiscale challenges, which range from atomic-scale defect interactions to polycrystal-level crack paths, while identifying unresolved gaps in predictive accuracy for industrial applications.

2 Fundamentals of Ferroelectric Fracture

Fracture mechanics, emerging as a pivotal discipline starting from the 1940s, has evolved into a robust framework for analyzing material failure under multifield loading [12]. Its core principles, which characterize crack initiation, propagation, and ultimate structural failure under mechanical stress, thermal gradients, defects, and electromechanical coupling, provide the foundation for assessing fracture behavior in complex materials such as metals and alloys, polymers, and ceramics. For ferroelectrics, this framework quantifies how coupled electric fields and mechanical stresses govern crack dynamics, with the fundamental objective of predicting failure to ensure the reliability of ferroelectric devices.

To address the complex fracture challenges in ferroelectric and piezoelectric materials, a multidimensional analytical framework has been developed that integrates methods from classical fracture mechanics with adaptations for electromechanical coupling. Linear elastic fracture mechanics (LEFM) provides quantitative models for crack propagation in brittle elastic materials under small-scale yielding conditions [13,14]. Still, its application to ferroelectrics is limited due to nonlinear effects like domain switching and electric field-induced phase transformations. For materials that exhibit inelastic deformation, elastic-plastic fracture mechanics (EPFM) provides an accurate characterization of fracture behavior, analogous to domain-switching-induced plasticity in ferroelectrics under high stress [15]. Fatigue fracture analysis methods, through cyclic loading experiments, reveal failure mechanisms, crack growth rates, and fatigue life predictions, particularly relevant for ferroelectric actuators subjected to alternating electric fields [16]. Probabilistic models based on statistical mechanics effectively quantify the influence of microstructural defect distributions (e.g., pores, grain boundaries) on crack propagation paths, accounting for the inherent variability in polycrystalline ferroelectrics [17]. Additionally, numerical approaches, such as the boundary element method [18], XFEM [19] and PFM [20], provide high-precision simulation platforms for engineering fracture prediction by capturing crack-domain interactions and electromechanical coupling. These methods complement one another; for instance, combining LEFM with EPFM addresses fracture dynamics at high strain rates and complex stress states in ferroelectric ceramics [21], while integrating fatigue analysis with statistical methods improves reliability assessments of structural failure risk under cyclic loading in piezoelectric devices [22].

The transition from classical fracture mechanics to the specialized case of ferroelectric and piezoelectric materials requires theoretical frameworks that explicitly account for electromechanical coupling. The fracture behavior of these materials is governed by a complex interplay between mechanical stresses, electric fields, and inherent material anisotropy, which classical theories cannot fully describe. This section establishes the foundational concepts by examining three critical, interconnected aspects that span multiple length scales. First, LPFM extends classical theory by incorporating electrical variables and defines coupled mechanical and electrical intensity factors to characterize the crack-tip field. However, its predictive capability is often limited by discrepancies with experimental observations. Second, the phenomenon of Fracture Toughness Anisotropy and Size Effects is analyzed, arising from poling-induced crystallographic texture and

domain-switching processes at the crack tip, which are strongly dependent on microstructural dimensions. Finally, at smaller scales where significant strain gradients exist, the Crack-tip Flexoelectric Effect, a direct coupling between strain gradients and polarization, becomes non-negligible, generating localized electric fields that substantially influence the fracture energy. Together, these aspects form a multi-scale analytical framework, from continuum-level LPFM to microstructurally informed anisotropy, down to nanoscale flexoelectricity, which is essential for accurately predicting the fracture resistance of ferroelectric materials.

Fig. 1 provides a comprehensive experimental overview of these ferroelectric fracture characteristics, showcasing phenomena such as domain-switching-induced crack branching, domain wall movements, and the critical role of domain-wall interactions in determining the macroscopic failure mode. The detailed description on LPFM and the other fracture mechanisms in ferroelectrics is elucidated in the following subsections.

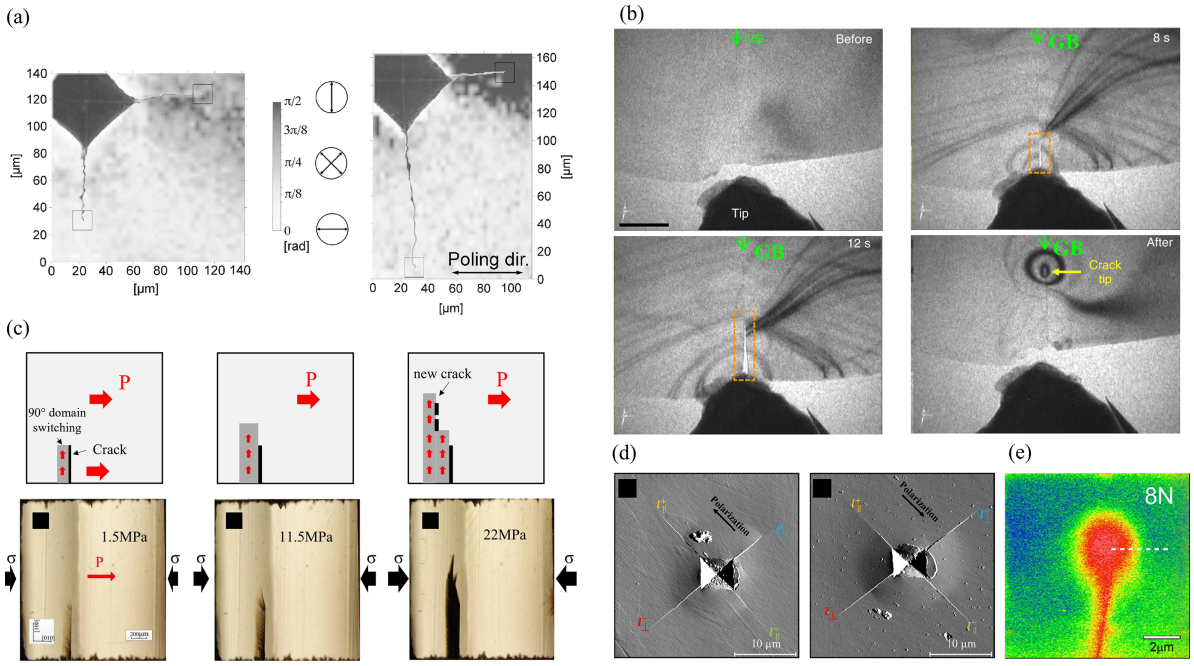

Figure 1: Distinctive fracture mechanisms in ferroelectric materials, arising from their coupled electromechanical response and microstructural features. (**a**) **Fracture toughness anisotropy:** Crack propagation length varies with orientation relative to poling direction in barium titanate single crystals, demonstrating direction-dependent toughness [23]. (**b**) **Grain boundary effects:** Cracks in metallic ceramics preferentially propagate along grain boundaries, highlighting the role of microstructure in determining the fracture path [24]. (**c**) **domain switching effect:** New crack forms at the 90 ° domain switching zone under a compressive loading [25] (**d**) **Flexoelectric fracture ratchet:** The crack-tip flexoelectric effect induces asymmetry, resulting in different crack lengths for propagation parallel vs. anti-parallel to polarization direction [26]. (**e**) **Crack-tip potential distribution:** The flexoelectric effect significantly distorts the electric potential field near a crack tip, influencing local driving force for fracture [27].

2.1 Linear Piezoelectric Fracture Mechanics

Linear fracture mechanics formulations for piezoelectric materials must account for electromechanical coupling, a fundamental aspect distinguishing them from conventional LEFM. This subsection outlines the foundational framework of LPFM for homogeneous materials. The formulation explicitly accounts for inherent electromechanical coupling and anisotropy. To facilitate derivation of closed-form analytical solutions for static cracks, the model deliberately neglects nonlinear micromechanical origins, such as domain wall motion

and other microstructural features inherent to ferroelectric behavior. This simplification establishes an essential theoretical baseline for analyzing crack-tip fields under purely linear electromechanical conditions. General reviews of the current state of LPFM can be found in books by Fang and Liu [28] and Qin [29].

The electromechanical behavior of a ferroelectric material is governed by the fundamental equations of electrostatics and mechanics. Hereafter, Einstein notation is implied, Latin indices $ijkl$ run through spatial dimensions, and commas in subscripts denote spatial partial differentiation. Assuming small deformation, mechanical strain tensor ε_{ij} derives from mechanical displacement vector u_i

$$\varepsilon_{ij} = \frac{1}{2}(u_{i,j} + u_{j,i}). \tag{1}$$

The electric field vector E_i derives from electric potential ϕ by

$$E_i = -\phi_{,i}. \tag{2}$$

Denote the space occupied by a ferroelectric medium and its boundary by $\mathcal{B}$ and $\partial\mathcal{B}$, respectively. At each point in $\mathcal{B}$, mechanical equilibrium

$$\sigma_{ij,i} + f_j = 0 \quad \text{in } \mathcal{B} \tag{3}$$

must be satisfied, where σ_{ij} is Cauchy stress in Cartesian space and f_i is the body force in ith direction. The equilibrium condition requires appropriate boundary conditions, either displacement-controlled or traction-controlled, i.e.,

$$u_i = \bar{u}_i \quad \text{on } \partial\mathcal{B}_u, \tag{4}$$

$$\sigma_{ij}n_j = \bar{t}_j \quad \text{on } \partial\mathcal{B}_\sigma. \tag{5}$$

The electric quantities, such as electrical displacement D_i and volume charge density q, follow quasi-static equilibrium derived from Maxwell's equations in matter, i.e.,

$$D_{i,i} = q \quad \text{in } \mathcal{B}. \tag{6}$$

Here, the quasi-electrostatic approximation is assumed. At the boundaries, electric quantities satisfy

$$\phi = \bar{\phi} \quad \text{on } \partial\mathcal{B}_\phi, \tag{7a}$$

$$D_i n_i = -\bar{\omega} \quad \text{on } \partial\mathcal{B}_D, \tag{7b}$$

where ϕ is the electric potential and $\bar{\omega}$ is the surface charge density.

Linear piezoelectric constitutive equations couple the mechanical and electrical fields. These equations derive either from experimental observations or thermodynamic theory. In the adiabatic state, independent dual variables of piezoelectric materials take four forms: ε_{ij}-D_i, ε_{ij}-E_i, σ_{ij}-D_i and σ_{ij}-E_i. Corresponding thermodynamic functions are the internal energy density ($\mathcal{U}$), electrical enthalpy density ($\mathcal{H}^e$), mechanical enthalpy density ($\mathcal{H}^m$) and enthalpy density ($\mathcal{H}$). For instance, $\mathcal{H}$, commonly used in finite element functional construction, is defined as

$$\mathcal{H}^e(\varepsilon_{ij}, E_i) = \frac{1}{2}(\sigma_{ij}\varepsilon_{ij} - D_i E_i). \tag{8}$$

According to the first law of thermodynamics, in an adiabatic state, variance in the internal energy density of a piezoelectrics equals the microwork done by mechanical load and electric field. By Legendre transformation, total differential of electrical enthalpy becomes

$$\mathrm{d}\mathcal{H}^e(\varepsilon_{ij}, E_i) = \mathrm{d}\mathcal{U} - D_i \mathrm{d}E_i = \sigma_{ij}\mathrm{d}\varepsilon_{ij} + E_i \mathrm{d}D_i - D_i \mathrm{d}E_i. \tag{9}$$

Implicit piezoelectric equations follow sequentially

$$\sigma_{ij} = \frac{\partial \mathcal{H}^e}{\partial \varepsilon_{ij}}, \tag{10}$$

$$D_i = -\frac{\partial \mathcal{H}^e}{\partial E_i}. \tag{11}$$

For a linear piezoelectric material, electrical enthalpy density is

$$\frac{1}{2} c_{ijkl}\varepsilon_{ij}\varepsilon_{kl} - e_{kij}\varepsilon_{ij}E_k - \frac{1}{2}\kappa_{ij}E_iE_j, \tag{12}$$

where, c_{ijkl}, e_{kij}, and κ_{ij} are respectively the elastic stiffness tensor, piezoelectric stress tensor, and dielectric tensor. These tensors are not necessarily isotropic. Substituting Eq. (12) into Eq. (10) yields the piezoelectric constitutive relation:

$$\sigma_{ij} = c_{ijkl}\varepsilon_{kl} - e_{kij}E_k, \tag{13}$$

$$D_i = e_{ikl}\varepsilon_{kl} + \kappa_{ij}E_j. \tag{14}$$

Other constitutive equations relating the remaining independent dual variables can be derived analogously; see Fang and Liu [28].

Piezoelectric fracture theory based on LEFM was pioneered by Parton [30], building on Irwin's fracture theory for plates [31]. In Parton's theory of a crack in a piezoelectric plate, crack thickness is assumed small, and the electric displacement and potential on its upper and lower surfaces are equal:

$$\phi^+ = \phi^-, \tag{15}$$

$$D_n^+ = D_n^-, \tag{16}$$

where the superscripts denote the field quantities of the upper and lower surfaces, and the subscript $[\,]_n$ denotes the component in the normal direction from the crack surface. This boundary condition is termed permeable, and the corresponding crack is called a permeable crack. Heyer et al. [32] examined this model using NaCl solution to fill crack gaps in piezoelectric materials to satisfy these criteria. In 1980, Deeg proposed an impermeable crack model. Since air or vacuum permittivity inside the crack gap is approximately 1000 times smaller than commercial lead zirconium titanate (PZT) ceramics, some researchers considered it zero (charge-free). However, McMeeking [33] pointed out that the impermeable crack model was physically unrealistic. The third type model (PKHS) accounting for permittivity of the medium inside the crack gap was proposed independently by Parton and Kudryavtsev [34] and Hao and Shen [6]. The PKHS model assumes a dielectric medium with finite permittivity inside the crack gap, as shown in Fig. 2. As illustrated in Fig. 2, a through crack with the propagation length of a is present. The crack surfaces are denoted as S^+ and S^-, with a crack opening displacement Δu. A potential drop Δ across the crack induces an electric field inside the crack in the x_2-direction. A polar coordinate system (r, θ) is introduced, where r is the distance from the crack front and θ is the angle measured from the x_1-axis. The specimen is subjected to remote loading,

which includes a uniform far-field stress σ_{22}^{∞}, a uniform far-field dielectric displacement D_2^{∞} or a uniform far-field electric field E_2^{∞}. The dielectric displacement on the top and bottom crack surfaces is governed by the relation (boundary condition):

$$D_2^+(x_1) = D_2^+(x_1), \tag{17}$$

$$D_2^+(u_2^+ - u_2) = \kappa_m(-\phi^+ - \phi^-), \tag{18}$$

where κ_m is permittivity of the medium inside the crack.

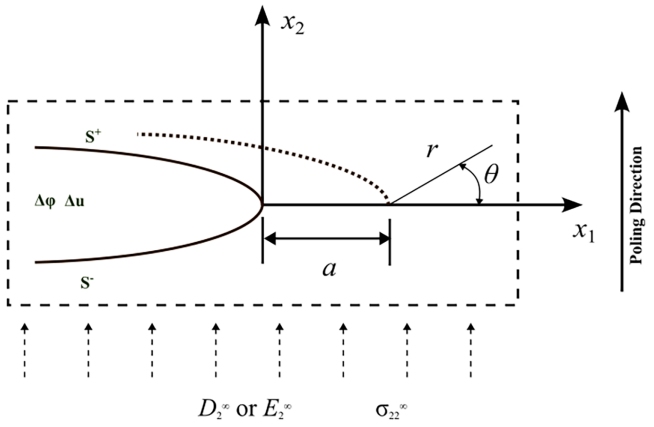

Figure 2: Schematic illustration of the crack in a piezoelectric medium.

The permittivity κ_m equals to $\epsilon_0 = 8.85 \times 10^{-12}$ C/Vm, if the cracked piezoelectric material is put into the vacuum or air, and would be infinite if the crack is filled with a conducting solution (e.g., NaCl solution). The PKHS model (sometimes regarded as semi-permeable crack) generalizes crack-face boundary conditions in piezoelectric fracture mechanics, with permeable and impermeable crack models emerging as its two limiting cases. These limits correspond to the crack being filled with a perfectly conducting medium (permeable) or a vacuum (impermeable), respectively.

For a constant mechanical far-field stress σ_{22}^{∞} and electrical far field E_2^{∞} loading on an infinite transversal isotropic piezoelectric material with a 2D crack poled in x_2 direction (i.e., material polarization $\mathbf{P} = (0, P_r, 0)$). The J-integral is calculated by [35]

$$J_1 = \int_S Q_{1i} n_i \mathrm{d}s + \frac{\kappa_v (\phi^+ - \phi^-)^2}{2\delta}, \tag{19}$$

where, S_a is an arbitrary outer contour of the crack in the piezoelectric material region, n_i is the outward unit normal, and Q_{ij} is the generalized energy-momentum tensor given by

$$Q_{ij} = \frac{1}{2}(\sigma_{ij}\varepsilon_{ij} - D_i E_i)\delta_{ij} - \sigma_{kj} u_{k,i} - D_j \phi_i. \tag{20}$$

Detailed analytical solutions for displacement and electric field distribution, normal crack opening displacement jump and electric potential drop across the crack gap are examined by Ou and Chen [36]. Mcmeeking [37] and Landis [38] noted a difference between total energy release rate (ERR) and crack ERR due to the energy stored in the medium inside the PKHS crack. For semi-permeable boundary condition, total ERR is

$$G^{\text{total}} = G^{\text{crack}} - \frac{1}{4}\kappa_v \frac{\Delta\phi^2}{\Delta u}, \tag{21}$$

where $\Delta\phi$ and Δu are potential gap and displacement gap at the crack tip.

The three crack types above assume the crack interior is filled with an insulating medium. A conducting crack also exists, where potential is identical on the crack surface. This allows free charges to move, with positive and negative charges accumulating at crack tips. Conductive crack paths can form when partially detached metallization coats fracture surfaces, as often occurs in layered composites and multilayer devices. Embedded electrodes in ceramics provide another example. Suo et al. [13] calculated ERR of an electrically conducting crack as $G^{\text{cond}} = 2\kappa_v U^2 d^{-1}$. The electric field in the ceramic becomes singular ahead of the crack tip and is quantified by the electric field intensity factor:

$$K_E = \lim_{r\to 0} \sqrt{2\pi r} E_2(r, \theta = 0). \tag{22}$$

Fig. 3 summarizes and contrasts three primary electrical boundary condition models for a crack within the LPFM framework. It schematically illustrates the permeable, impermeable, and conducting crack models, highlighting their distinct assumptions regarding the dielectric displacement and electric potential across the crack surfaces.

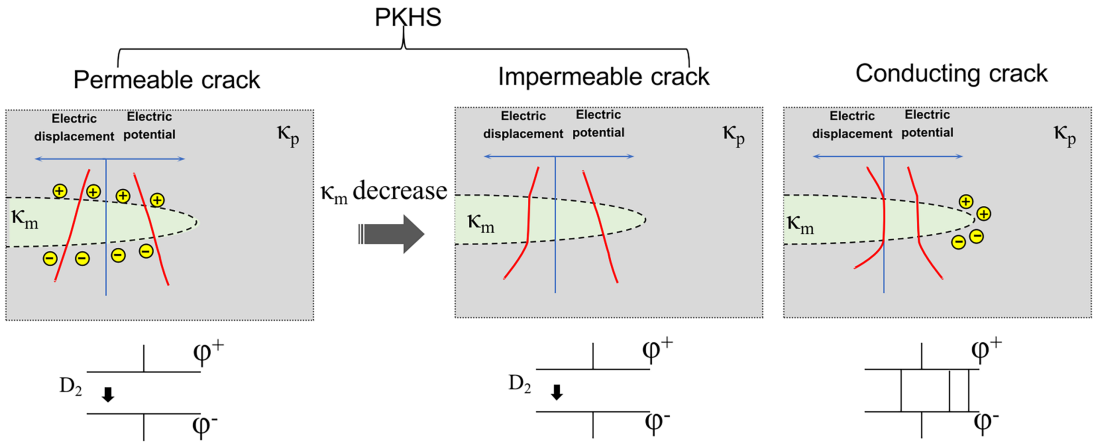

Figure 3: Schematic illustration of different types of cracks and the corresponding electric displacement and potential distribution.

The LPFM framework provides an essential foundation and analytical tools for understanding crack-tip fields and predicting fracture initiation under small-scale switching conditions. A key advantage over classical linear elastic fracture mechanics (LEFM) is its ability to account for both the electric field and the linear electromechanical coupling at the crack tip. Its utility remains paramount for problems where material nonlinearity and microstructural evolution are negligible. Indeed, LPFM has played a foundational role in the theoretical analysis of fracture in ferroelectric materials over the past decades. Its primary contributions include establishing the fundamental framework for analyzing crack-tip electromechanical fields under combined loading [39], and serving as the basis for analyzing phenomena such as electric-field-induced crack closure [40]. Furthermore, LPFM provides the essential linear elastic field solutions that underpin more advanced "small-scale" nonlinear models, which attempt to account for localized domain switching at the crack tip by superimposing it onto the linear solution.

However, it is critical to recognize that LPFM is fundamentally a quantitative analytical tool for calculating K_c and ERR, not an intrinsic predictor of failure criteria. Its formulations rely on externally determined critical parameters (e.g., fracture toughness) and cannot, on their own, define the conditions for crack initiation or propagation. This intrinsic limitation becomes starkly apparent when LPFM predictions contradict key experimental observations, most notably its failure to explain crack growth under purely electrical loading. Consequently, LPFM must be synergistically integrated with experimental characterization, such as fracture testing under combined electromechanical loads and *in situ* observation of crack-tip processes, to calibrate its parameters and provide a holistic, experimentally validated interpretation of ferroelectric fracture behavior.

On the other hand, LPFM shows its limitations when dealing with nonlinear effects caused by ferroelectric domain switching. Firstly, it cannot model the nonlinear, hysteresis domain switching processes that occur at the crack tip, which fundamentally alter the local driving force for fracture. Secondly, it treats the material as a homogeneous continuum, failing to account for the microstructure-dependent fracture behavior influenced by grain boundaries, domain wall movement, and local polarization variants. Thirdly, it fails to predict the piezoelectric fracture behavior under large electric field, where nonlinear response emerges. It is precisely these limitations that motivate the development of the non-linear piezoelectric fracture theory, especially the models considering domain switching.

2.2 Fracture Toughness Anisotropy

Fracture toughness of poled ferroelectric ceramics exhibits pronounced anisotropy, consistently observed across different testing methodologies. Early studies using the Vickers indentation crack length (ICL) method revealed marked differences in crack lengths depending on orientation relative to poling direction [21,41,42]. For instance, in PZT PIC 151, cracks propagating parallel to poling direction are significantly shorter than those propagating perpendicular to it, indicating higher fracture toughness for the former orientation. Controlled fracture mechanics specimens, such as compact tension (CT) tests measuring full resistance curves (R-curves), later confirmed the anisotropy of the material [9,43]. These studies showed that samples poled parallel to intended crack growth direction exhibited highest toughening, while poling perpendicular to crack plane resulted in minimal R-curve behavior, with unpoled samples showing intermediate values. Oates et al. [44] further investigated R-curves of PZT-PIC 151 ceramics with CT specimens for different poling directions. Fracture resistances at R-curve plateaus differed for poling along the thickness, crack growth, and loading directions. The experiment on the compact-tension barium titanate and PZT-PIC 151 indicate that electric field increases initial and plateau values of R-curve and shortens the curves [43].

The experimental consensus on fracture toughness anisotropy in ferroelectrics has motivated rigorous investigations into the underlying physical mechanisms, with flexoelectricity at the crack tip emerging as a key explanatory factor. This mechanistic understanding is schematically summarized in Fig. 4. Fig. 4a illustrates the mechanism of ferroelectric fracture toughness anisotropy: a crack propagating parallel to the spontaneous polarization (P_s) is significantly shorter than one propagating perpendicular to it due to the electromechanical coupling effect. Fig. 4b presents the experimental evidence for the ferroelectric fracture anisotropy. The crack growth resistance values are different at varies temperature for cracks propagating parallel and perpendicular to the poling direction in PZT ceramics, demonstrating that the polarization direction strongly affects the fracture toughness [23]. Crucially, this anisotropy manifests not only in the crack propagation direction relative to P_s (parallel vs. perpendicular) but also in its direction along the poling axis (parallel vs. anti-parallel). The latter is schematically illustrated in Fig. 4c, where the intense strain gradient at the crack tip induces a flexoelectric polarization (P_{fx}). The relative alignment between P_{fx} and

P_s modifies the local crack-driving force, via either crack-tip shielding or anti-shielding, thereby dictating the effective fracture toughness. This polarity-dependent mechanism, known as the flexoelectric fracture-ratchet effect, finds direct experimental validation in Fig. 4d, which shows a measurable difference in fracture toughness distribution for opposite polarization states [26].

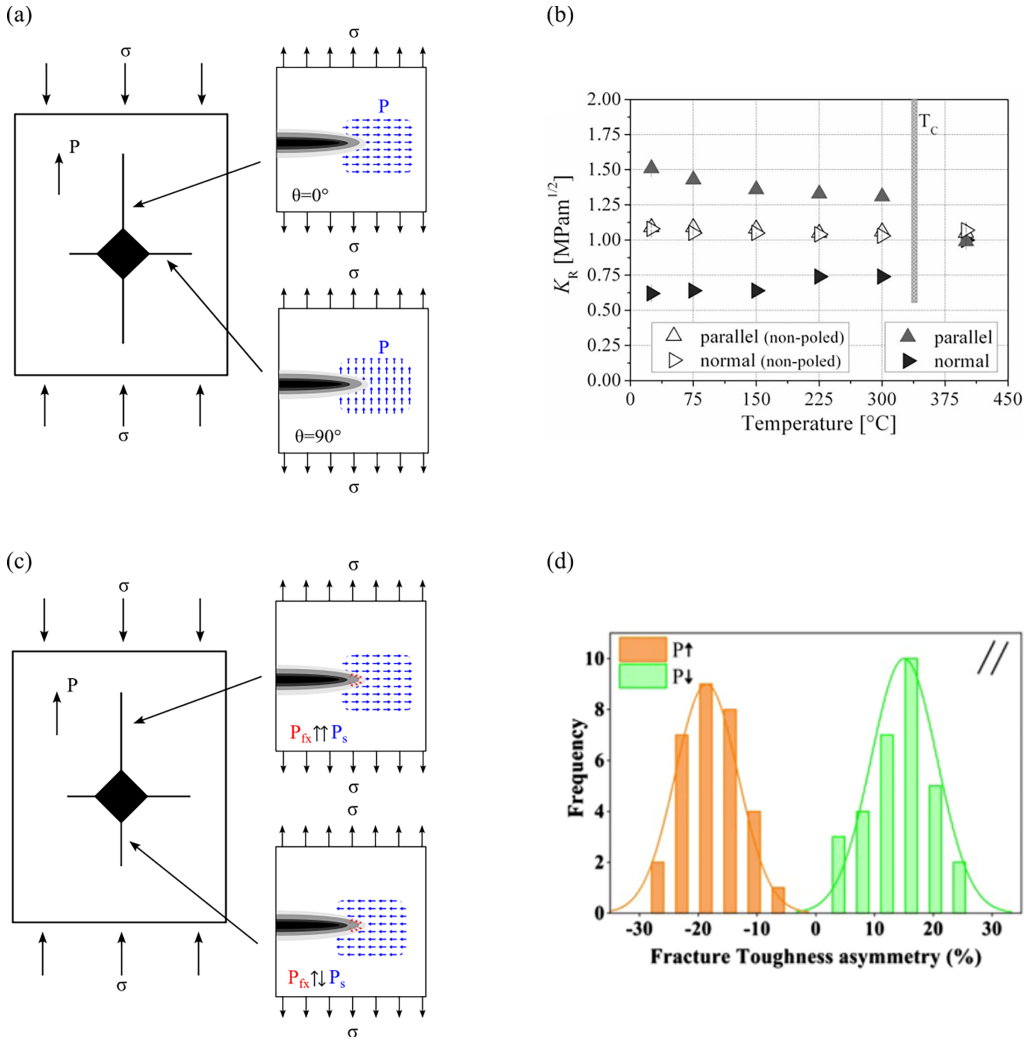

Figure 4: (**a**)Schematic figure of fracture toughness anisotropy caused by spontaneous polarization: The length of the crack parallel to the spontaneous polarization is longer than the one perpendicular to the spontaneous polarization. (**b**) Experimental evidence of the crack growth resistance (calculated from the fracture toughness) anisotropy in lead zirconium titanate specimens at different temperature [23] (**c**) Schematic figure of fracture toughness anisotropy caused by flexoelectric effect. (**d**) Histogram of fracture toughness asymmetry for cracks parallel and anti-parallel to the spontaneous polarization shows different anisotropy mechanism (flexoelectric fracture-ratchet effect) compared to the ferroelectric effect [26].

2.3 Grain Size Effect, Domain Switching and Other Factors

Fracture toughness of ferroelectric ceramics depends strongly on microstructural scale, particularly grain size. Systematic studies on materials such as PZT [45] demonstrate that coarse-grained ceramics exhibit significantly higher fracture toughness and more pronounced R-curve behavior compared to fine-grained counterparts [46]. This behavior is attributed to a shift in dominant fracture path: in coarse-grained

materials (e.g., grain size approx.30 μm), cracking tends to be transgranular (through grains), promoting more extensive domain switching in larger, less-constrained grain volumes ahead of the crack. Conversely, in fine-grained ceramics, fracture often proceeds along intergranular (grain boundary) paths, constraining development of large-scale domain-switching zones and limiting toughening [47]. The domain switching zones are experimentally determined by Mao and Fang [48] (See Fig. 5). When the poling direction is parallel to the crack propagation direction ($\Phi = 0°$), the switching zone extends mainly ahead of the crack tip, whereas for $\Phi = 90°$, it becomes more symmetric around the crack. Compressive stress produces a much larger switching zone than tensile stress, indicating easier domain switching under compression. Under coupled electromechanical loading, different crack–poling orientations further lead to distinct asymmetric distributions and coexistence of 90° and 180° switching zones.

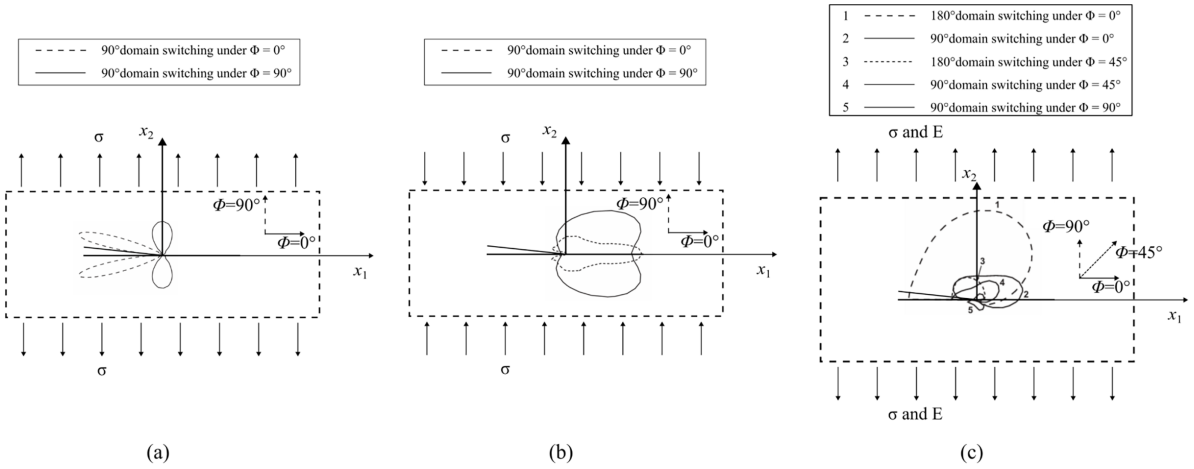

Figure 5: Domain switching zone is strongly dependent on the poling direction, stress state, and crack orientation: The shape of domain switching zones near ferroelectric crack tip under (**a**) a tension stress field; (**b**) a compressive stress field; (**c**) various initial poling directions.

The primary mechanism responsible for anisotropy and associated R-curve behavior is localized ferroelastic/ferroelectric domain switching at the crack tips. Domain switching is also key to nonlinear fracture behavior in ferroelectric materials. Modeling domain switching in ferroelectric materials constitutes a well-developed field essential for understanding nonlinear constitutive behavior. To describe nonlinear and irreversible electromechanical behavior inherent to ferroelectrics, diverse theoretical frameworks have been established. These range from phenomenological constitutive models with history dependence [49,50] and microscopic switching models based on energetical criterion [51,52], which track individual domain reorientations, to macroscopic constitutive models [53,54] and variational rate-dependent formulations [55,56], which describe the evolution of internal state variables on a continuum scale. At the most fundamental level, Landau-Devonshire theory and its spatially resolved extension, Landau-Ginzburg theory, provide a thermodynamic basis for modeling domain evolution and will be discussed in detail in the following section [57,58].

The highly concentrated tensile stress field ahead of a propagating crack can induce irreversible 90° reorientation of ferroelectric domains. Following the conceptual approach of models for transformation-toughened materials, several fracture models for ferroelectrics incorporating domain switching effects have been proposed [59–63].

Wang and Ricoeur proposed a fracture process zone in ferroelectrics [64]. Domain switching creates a transformation or process zone surrounding the crack, where the remanent strain perpendicular to the

crack faces induces compressive stresses. Direct experimental evidence for this zone comes from techniques mapping both switched domain distribution and resulting mechanical responses. X-ray microdiffraction and piezoresponse force microscopy has quantified domain reorientation near crack tips [65–67]. Atomic force microscopy has directly measured the associated "bump" in the crack opening displacement profile, corroborating predicted shielding stresses [68].

2.4 Crack-Tip Flexoelectric Effect

The flexoelectric effect, a linear coupling between strain gradients and electric polarization, emerges as a critical factor governing fracture behavior in ferroelectric materials at small scales where intense strain gradients exist near crack tips [69]. Fig. 6a shows the microscopic mechanism of net polarization induced by non-uniform strain. A strain gradient breaks local inversion symmetry, thereby generating a flexoelectric polarization via the separation of positive and negative charge centers. This extrinsic mechanism is fundamentally distinct from the intrinsic ferroelectric polarization caused by crystal asymmetry. The experimental evidence of such flexo-induced polarization could be found by visualizing the polarization distribution at crack tip based on a precisely manipulated transmission electron microscopy (TEM) observation (see also Fig. 6a) and graphical phase analysis (Fig. 6c).

Theoretical analysis reveals two key size-dependent phenomena: general enhancement of fracture resistance at the nanoscale and fracture toughness asymmetry contingent on polarization vector sign relative to crack propagation direct [70,71]. This asymmetry fundamentally breaks inversion symmetry in classical fracture mechanics of polar materials, with polarization-aligned directions typically exhibiting lower toughness. Direct experimental evidence for enormous local fields generated by this mechanism comes from atomic-scale observations, measuring giant flexoelectric polarization of ~62 μC cm^{-2} around crack tips in $SrTiO_3$ epitaxial films, confirming the crack tip as an intense flexoelectric sources [72] (Fig. 6b). Indentation experiments on periodically poled ferroelectrics have directly measured this flexoelectric fracture-ratchet effect, demonstrating asymmetric crack lengths confirming polarization acts as a switchable "valve" for crack propagation [26].

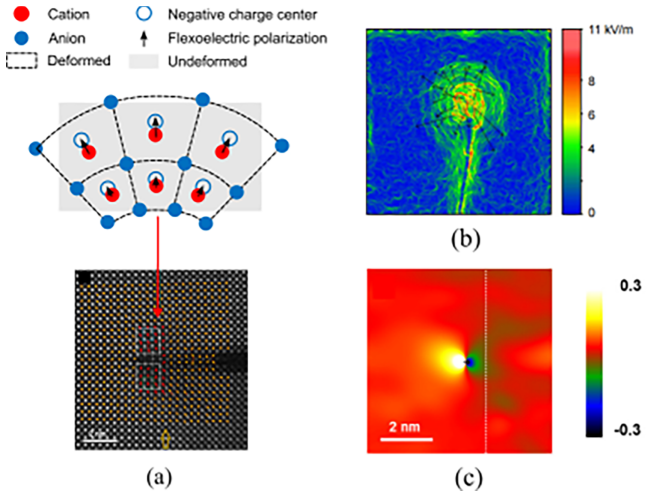

Figure 6: (**a**) The flexoelectric effect caused by non-uniform deformation during crack propagation can generate a polarization field at the crack tip. The schematic diagram illustrates the mechanism of the flexoelectric effect [72]. (**b**) The high electric potential at the crack tip is mainly due to the flexoelectric effect [27]. (**c**) Flexoelectric effect can promote or inhibit crack propagation, leading to asymmetry in fracture toughness.

Phase-field modeling, seamlessly integrating fracture evolution with ferroelectric domain dynamics, has become the primary tool for unraveling complex mechanisms behind these observations. For instance, simulations on ferroelectric single crystals (e.g., $BaTiO_3$) show that the flexoelectric effect significantly disrupts crack-tip domain configurations, leading to asymmetric domain switching zones that influence fracture driving forces [73]. These models demonstrate that the flexoelectric effect alters both crack propagation rate and path. Whether the specific influence accelerates or impedes growth is highly sensitive to the initial polarization direction and the sign of the flexoelectric coefficients [74,75]. When the crack propagation is parallel to the polarization, the crack extends faster and at a lower load, whereas antiparallel propagation is delayed, effectively modulating the apparent fracture toughness [74]. For cracks propagating perpendicular to polarization, flexoelectric effect primarily induces the crack path deflection rather than changing initiation load, with cracks tending to kink towards the direction antiparallel to the polarization [74,76]. This path deflection is attributed to flexoelectricity-induced eigenstrain creating asymmetric stress field, locally shielding or anti-shielding crack tip.

From a computational mechanics perspective, the phase-field method has been extended to rigorously dissect the crack-tip flexoelectric effect. A key advancement is the development of a unified phase-field framework that couples ferroelectric domain evolution with both strain gradient elasticity (SGE) and flexoelectricity within a single variational formulation [77]. Its core methodological innovation lies in a novel mixed finite-element scheme designed to isolate and quantify the individual roles of SGE and flexoelectric coupling. Parallelly, a distinct numerical strategy has been established to efficiently integrate flexoelectricity into ferroelectric phase-field models. This approach employs a Gaussian-point interpolation technique to compute strain gradients, thereby circumventing the need for high-order shape functions and enabling simulations with standard C^0-continuous finite elements [78]. Together, these works reflect the ongoing refinement in computational mechanics—progressing from models that couple fracture and ferroelectric domains to frameworks that provide essential tools for analyzing high-order effects such as strain gradient effect and flexoelectric effect at ferroelectric crack tips.

In summary, crack-tip flexoelectric effect is a potent size-dependent mechanism introducing anisotropy into ferroelectric fracture process. It can induce toughness asymmetry, dictate crack propagation paths, and modulate growth kinetics through dynamic interplay with polarization. Accurately predicting fracture in modern miniaturized ferroelectric devices therefore requires explicit incorporation of this effect into constitutive models.

3 Typical Approaches for Modeling Fracture

Accurate numerical modeling of fracture, particularly prediction of crack initiation and propagation paths, remains a significant challenge in computational mechanics. This challenge is amplified for ferroelectric and piezoelectric materials due to inherent coupling between mechanical deformation and electric fields. To address this, various computational frameworks have been developed, broadly categorized by how they represent crack displacement discontinuity. Traditional methods often rely on explicit geometric descriptions that tie crack paths to computational meshes. Examples include the CZM (with interface elements inserted along predefined paths) and other mesh-dependent techniques like element deletion [79–81]. These methods, while computationally efficient for certain scenarios, can suffer from mesh-dependent crack paths and difficulties handling complex, three-dimensional, or branching crack systems without extensive remeshing.

To overcome these limitations, advanced non-geometric description methods have emerged, allowing cracks to propagate independently of the underlying meshes. The XFEM is a prominent example, enriching displacement fields with discontinuous functions to represent cracks implicitly [82]. The phase-field approach has gained considerable attention for its ability to handle complex crack topologies, including

crack nucleation, branching, and merging, without requiring explicit crack tracking or adaptive remeshing, making it particularly suitable for simulating fracture in the complex, evolving microstructures of ferroelectric materials. This section provides concise overviews of these two established methodologies—the CZM (Section 3.1) and eXtended Finite Element Method (Section 3.2)—before focusing in detail on the Phase-Field Method (PFM) for fracture (Section 3.3). The comparison between CZM, XFEM and PFF are illustrated in Fig. 7.

model	CZM	XFEM	PFM
Core principles	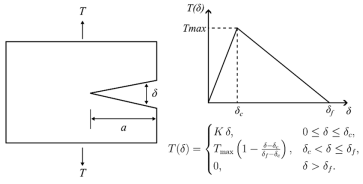	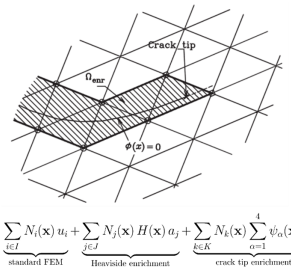	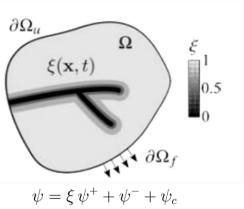
Crack representation	Cohesive zone ahead of the crack tip, governed by a traction–separation law. Effective for interfacial failure such as grain boundaries or electrode delamination.	Enriched shape functions capture strong discontinuities independently of the mesh. Suitable for cracks in piezoelectric structures.	Crack is represented as a continuous field variable (phase field), where the crack evolution is governed by the phase field function.
Crack initiation and propagation	Crack path must be prescribed a priori. Limited to known interfaces or weak planes.	Arbitrary crack growth without remeshing. Handles initiation and propagation along complex paths.	Automatic nucleation and propagation. Naturally captures branching, merging, and crack–domain interactions.
Mesh requirements	High. Cracks are confined to element boundaries; mesh must align with expected path.	Moderate. Cracks are mesh-independent, but refinement near the tip is needed for accuracy.	Low. Fine mesh only required in diffuse crack region to resolve the length scale.

Figure 7: comparison between different numerical models for fracture.

3.1 The Cohesive Zone Model

The Cohesive Zone Model (CZM) provides a robust computational framework for simulating crack initiation and propagation by introducing a phenomenological traction-separation law along a prospective crack path. This law governs the gradual degradation of material cohesion, thereby removing the stress singularity associated with a sharp crack tip in classical fracture mechanics. A typical bilinear traction-separation response features an initial elastic regime up to a peak cohesive strength, followed by a linear softening branch. The area under this complete curve defines the fracture energy required for complete separation. Implementing theses laws within interface or cohesive elements in a finite element framework, the CZM can model complex fracture processes such as mixed-mode failure and crack growth along predefined paths without remeshing [83].

Applying CZM to ferroelectric fracture requires extensions capturing coupled electromechanical behavior and micro-mechanisms such as domain switching. A fundamental theoretical advancement was formulation of micromechanically informed cohesive laws, where fracture process zones are modeled as regions of stress- and electric-field-induced domain switching around crack tips. This approach directly links the switching zone geometry, which depends on the poling direction and applied field, to the apparent fracture toughness, establishing criteria under which toughness is a function of the electric field, $K_{IC}(E)$ [84]. For engineering applications such as ferroelectric multilayer actuators, advanced Electromechanical Cyclic Cohesive Zone Models (EMCCZM) have been developed to simulate damage initiation and accumulation

under cyclic electric loading [85]. Coupled simulations reveal that poling processes themselves can induce crack initiation at electrode edges due to high field concentrations, and subsequent in-service electric cycling drives progressive crack propagation and interface delamination [86]. The primary challenge remains accurately calibrating of multiparameter coupled traction-separation laws, which must capture the nonlinear, history-dependent response dictated by domain switching.

3.2 The eXtended Finite Element Method

The XFEM represents a paradigm shift in numerical fracture mechanics by enabling the simulation of arbitrary crack growth without requiring the finite element mesh to conform to the crack geometry. This is achieved through the concept of local enrichment, where the standard finite element displacement approximations are augmented with additional functions. The discontinuous Heaviside function models displacement jumps across crack faces, and asymptotic crack-tip functions capture the singular stress/electromechanical fields near the tip. Crack geometry is typically tracked independently using level set functions [87]. The methodology extends beyond isotropic materials to more complex systems, such as orthotropic functionally graded materials [88], composites, and biomaterials [89], demonstrating broad applicability in multifield fracture mechanics. This collective work underscores XFEM as a preferred numerical methodology for material engineering involving complex crack geometries, dynamic loading, material interfaces, and inverse design.

This framework enables the natural simulation of complex fracture events, including crack initiation, branching, and merging, which are challenging for methods such as CZM, which often require predefined crack paths. It is crucial to distinguish their fundamental roles: CZM is a phenomenological constitutive model that describes the traction-separation behavior in a fracture process zone, whereas XFEM is a numerical discretization framework designed to handle strong discontinuities within a standard finite element setting. They are complementary and can be combined. For instance, cohesive laws describing crack-face behavior can be applied within XFEM formulations. Advanced variants, such as Cell-Based Smoothed XFEM (CS-XFEM), have been developed to improve accuracy by transforming domain integration into boundary integration, simplifying stiffness matrix computation, and avoiding derivatives of the singular crack-tip enrichment functions [90].

Applying XFEM to ferroelectric and piezoelectric fracture requires coupling with electromechanical constitutive laws, and it has proven exceptionally versatile for tackling various coupled problems. For dynamic fracture analysis, XFEM has been employed to study transient response of cracked piezoelectric plates under electromechanical impact, calculating dynamic stress and electric displacement intensity factors using dynamic interaction integrals [91]. In crack repair and active control, XFEM simulations model effectiveness of bonded piezoelectric patches and analyze how parameters such as patch shape, adhesive properties, and applied voltage influence reduction of stress intensity factors at crack tips in host structure [92]. XFEM also serves as a tool for defect detection and inverse analysis. Coupling XFEM with optimization algorithms enables identification the locations, sizes, and orientations of multiple embedded cracks or flaws in piezoelectric structures from measured electromechanical responses [93]. A particularly significant application is analysis of interfacial cracks in piezoelectric bimaterials, where specialized enrichment functions accounting for oscillatory singularities at the interface must be implemented [89].

3.3 The Phase-Field Method for Fracture

Phase-Field Method (PFM) for fracture represents a fundamental shift from methods that explicitly track discrete cracks towards a continuous, variational description of crack evolution. Its theoretical cornerstone is the variational framework for brittle fracture, reformulating Griffith's criterion [94] as a global

energy minimization problem, naturally enabling prediction of crack initiation and complex propagation paths without *a priori* knowledge of the crack trajectory [95]. Practical implementation of this framework was achieved through regularization via Γ-convergence, introducing a continuous scalar phase-field (or damage) variable $d(\mathbf{x})$ to smear the sharp crack discontinuity over finite widths controlled by length scale parameter l [19].

A thermodynamically consistent numerical framework for PFM was subsequently established. This framework defines total energy functional as sum of the stored elastic energy (degraded by the phase field), crack surface energy (approximated by a functional of d and ∇d), and the work of external forces [96]. A critical innovation was the tensile-compressive split of the elastic energy density, ensuring only the tensile part contributes to the crack driving force, thereby preventing unphysical cracking under compressive loads [97]. To enforce crack irreversibility ($\dot{d} \geq 0$), a local history field $\mathcal{H}$ was introduced to record the maximum tensile energy density reached over time [98]. Coupled systems of mechanical equilibrium and phase-field evolution equations are typically solved using staggered (operator-split) solution scheme [98].

Inherent extensibility of this variational framework is one of its greatest strengths. It has been generalized to model dynamic crack propagation [99]. For materials with directional properties, models have been developed accounting for anisotropic fracture surface energy [100] and, separately, for full elastic anisotropy while maintaining tension-compression split [101]. Advanced numerical techniques, such as adaptive isogeometric analysis with T-splines, have efficiently resolved higher-order continuity requirements of strongly anisotropic models [102]. Beyond brittle fracture, the framework has been extended to cohesive [103] and ductile fracture [104] in elastoplastic solids. Most pertinently for this review, the framework has been successfully extended to coupled electromechanical fracture in piezoelectric/ferroelectric materials, where the phase field degrades the total electromechanical enthalpy [20,98,105].

Building upon its robust variational foundation, the PFM for fracture has seen significant refinement to address practical challenges in predictive simulation. Key research thrusts aim to enhance its numerical robustness, physical fidelity, and experimental credibility. A central challenge stems from the non-convexity of the underlying energy functional, which complicates the reliable computation of global energy minimizers corresponding to the physical crack path. Advanced energetic formulations, incorporating backtracking algorithms and two-sided energy inequalities, have been developed to drive numerical solutions toward these global minimizers, ensuring consistency with the variational theory [106]. Concurrently, the physical realism of the pre-failure response, critical for accurately modeling crack nucleation in brittle materials, has been scrutinized. Studies demonstrate that the choice of the degradation function $g(d)$ profoundly influences the pre-peak material behavior. Higher-order functions (e.g., cubic, quartic) yield a nearly linear-elastic response until the onset of fracture, a marked improvement over simpler quadratic forms that introduce artificial softening, thereby offering a more physically sound description of brittle fracture [107]. Ultimately, the predictive capability of the phase-field framework must be grounded in rigorous validation. Its maturity is evidenced by detailed quantitative comparisons with analytical solutions and, importantly, the successful reproduction of experimental crack paths and load-displacement curves in brittle solids, bridging the gap between computational models and physical reality [108]. These interconnected advances—in numerical algorithms, constitutive detail, and experimental validation—collectively strengthen the PFM as a reliable tool for modeling complex fracture processes.

4 PFM for Ferroelectricity

The PFM, established as a robust variational framework for fracture as detailed in Section 3.3, is fundamentally a multi-phase modeling paradigm for treating diffusive interfaces. Its core concept, the description of a system's state and its evolution through an order parameter field and a governing free energy functional, is remarkably generalizable [109]. While in fracture mechanics the order parameter distinguishes broken from intact material, this same conceptual framework can be directly extended to model evolution of other microstructural features by choosing physically relevant order parameters and constructing appropriate energy functionals. Historically, the PFM was first developed for predicting snowflake morphology (i.e., solidification process) [110], then grain growth [111], and ferroelectric/ferromagnetic domain switching [112,113], well before its adaptation to fracture mechanics. For ferroelectrics, the natural order parameter is the spontaneous polarization vector **P**, describing the local dipole orientation [114,115]. The corresponding theoretical foundation is Ginzburg-Landau-Devonshire theory [116], providing the phenomenological framework for modeling ferroelectric domain dynamics. In this context, the gradient energy term in the functional, analogous to its role in fracture, penalizes sharp interfaces and governs the formation and energy of domain walls. The model introduces the order parameter (Here we choose the spontaneous polarization vector, P as the order parameter. The distinction between spontaneous polarization and the material polarization is comprehensively expounded in Ref. [115]) and its gradient. The total free energy of the system, F, can be expressed as

$$F = F^{\text{bulk}}(P_i) + F^{\text{grad}}(P_{i,j}) + F^{\text{elas}}(P_i, u_i) + F^{\text{elec}}(P_i, E_i) \tag{23}$$

where $F^{\text{bulk}}(P_i)$ is the Landau free energy describing the homogeneous polarization state of the ferroelectric material; $F^{\text{grad}}(P_{i,j})$ is the gradient energy, signifying that the polarization direction cannot change abruptly in space and forms the physical origin of domain wall formation; $F^{\text{elas}}(P_i, u_i)$ is the elastic strain energy; $F^{\text{elec}}(P_i, E_i)$ is the electric energy. Once the free energy is constructed, the evolution of the order parameter and domain structure of ferroelectric materials can be obtained by solving the time-dependent Ginzburg-Landau equation:

$$\frac{\partial P_i}{\partial t} = -M\frac{\delta F}{\delta P_i}, \tag{24}$$

where M is the kinetic parameter of the equation, which describes the mobility of the progress. This kinetic equation ensures that the spontaneous polarization evolves in a direction that reduces the total free energy.

The framework described above, specifically the total free energy functional and the evolution equation for polarization, provides the foundation for modeling fracture in ferroelectrics. Extending the functional shown in Eq. (23) to incorporate crack phase-field variables and corresponding energy contributions couples crack evolution seamlessly with ferroelectric domain evolution, establishing a unified PFM for ferroelectric fracture. Details of this coupled formulation, including specific forms of fracture energy functional and the interplay between crack propagation and domain switching, will be the focus of the following section.

Readers are referred to review papers [57,117] for detailed discussions of historical development and recent progress in ferroelectric phase-field models.

5 Phase-Field Modeling of Ferroelectric Fracture

The PFM has emerged as the predominant computational framework for modeling fracture in ferroelectric materials, primarily because it seamlessly integrates the evolution of a diffuse crack with complex, nonlinear evolution ferroelectric domain evolution within a unified variational formulation. Recent advancements have focused on extending the core coupled electromechanical fracture model to address several frontier challenges. These include integrating explicit microstructural features like grain boundaries and polycrystalline morphology to study transgranular vs. intergranular cracking; modeling the competition between crack growth and dielectric breakdown in high electric fields; simulating fatigue fracture under cyclic electromechanical loading to predict lifetime and damage accumulation; and leveraging ML techniques to accelerate simulations, optimize microstructures, or discover constitutive laws. Fig. 8a shows the evolution of ferroelectric PFF model. The following subsections review recent progress in each of these directions.

5.1 Fracture Model Coupled with Microstructure in Ferroelectrics

The various properties of ferroelectric materials, such as mechanical, electrical, and thermal (e.g., electrocaloric effect) properties, are largely determined by the distribution of their internal microstructure [118]. For ferroelectrics, microstructure includes grains and grain boundaries in ceramics, ferroelectric domains and domain walls within grains, cracks and other defects. (See Fig. 9a) These microstructures are intercoupled and collectively regulate polarization distribution and switching, thereby influencing its macro-scale nonlinear responses.

Ferroelectric domains are microscale regions within grains exhibiting uniform spontaneous polarization direction, representing the most fundamental microstructure in ferroelectrics. The interfaces between adjacent domains with different orientations are called a domain wall, with typical types including 180° and 90° domain walls. During the crack propagation process in ferroelectric materials, domain switching (particularly 90° domain switching) affects the fracture toughness and material brittleness.

Most ferroelectric devices are typically used as ceramics, meaning they consist of numerous individual crystalline units called grains. Polycrystalline states in ferroelecetrics adds an additional parameter that influences the domain structure within the single crystal grains, i.e., grain size. Single crystal grains have unique orientations, while for polycrystallined grain boundaries connect crystallites with different orientations, implying that polarization and lattice spacing continuity are rarely satisfied at grain boundaries. The variation in electromechanical properties with grain size is primarily attributed to mechanical stresses generated at the grain boundaries.

Crystal defects are disruptions of perfect periodic atomic arrangements within crystal lattices, mainly categorized as point, line, and planar defects. Common defects in ferroelectric materials include dislocations (line defects), oxygen vacancies (point defects), and cracks. These defect structures couple with the domain structure, thereby influencing the fracture behavior. For instance, dislocations can hinder or promote domain switching in ferroelectric thin films through pinning effects, thus affecting the fracture processes. Grain boundaries may hinder dislocation movement [119,120].

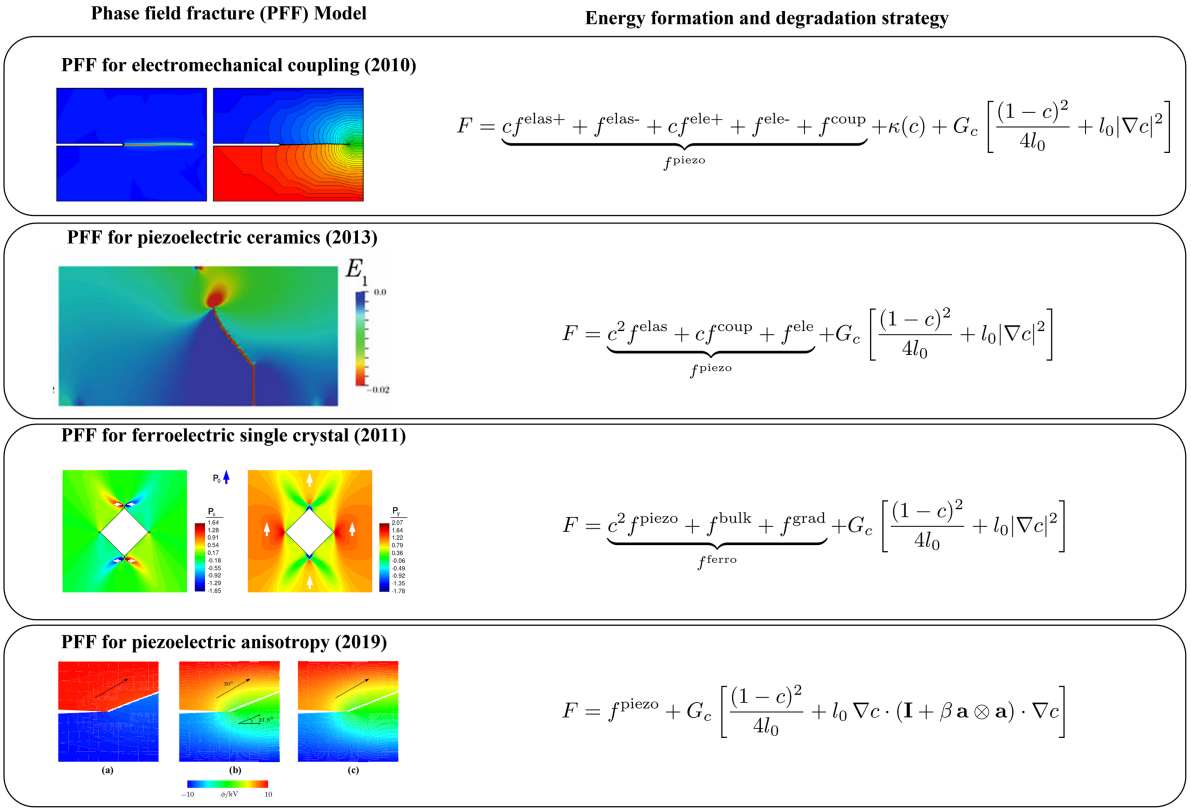

Figure 8: Review of phase field fracture (PFF) models for electromechanical coupling. The simulation results are adopted from Refs. [98,121–123]. The PFF model in the first row couples PFF to piezoelectricity, and the degradation function applies to part of the electrostatic energy; The PFF model in the second row degrade the electro-mechanical coupling term f^{coup}; By incorporating the Landau-Devonshire free energy, the PFF model in the third row establishes a framework for modeling coupled ferroelectric fracture. The PFF model in the fourth row is capable of simulating fracture anisotropy in piezoelectric single crystal by introducing an anisotropy tensor.

5.1.1 Grain and Grain Boundary

In ferroelectric polycrystalline materials, grains are fundamental units composed of a large number of periodically arranged atoms and possessing a specific crystal structure, see Fig. 9a. Grain size can be controlled through different synthesis routes [124]. Grain morphologies often differ across distinct material systems [125,126].

Grain boundaries are transition regions between two adjacent grains with different orientations, typically measuring from a few to dozens of atomic layers in width. Within this region, atomic arrangements show significant distortion and disorder relative to grain interiors, indicating defect structures. Dielectric constants, coercive fields, and remnant polarization correlate closely with grain size [127]. Grain boundaries also significantly influence the fatigue and fracture behavior of ferroelectric materials. Pohanka et al. [8] measured fracture toughness of single-crystal and polycrystalline $BaTiO_3$ above and below the ferroelectric Curie temperature. At 25°C in the ferroelectric state, increased fracture toughness with increasing grain size was observed. Within the grain size range of 1–150 μm, the fracture toughness of the material can vary by a factor of two. Li and Li further employed indentation crack length (ICL) methods to investigate the influence of microstructure on strength properties, verifying that below Curie temperature, fracture toughness of the material is related to the grain size [128]. However, ICL method has limitations, including the indentation

residual stresses biasing and issues related to semi-elliptical or hemispherical crack shapes. Meschke et al. [9] employed compact tension (CT) method to circumvent these limitations, revealing that grain size influences crack propagation paths: cracks primarily propagate transgranularly through coarse-grained regions and intergranularly through fine-grained regions. Similarly, Lugovy et al. [129] conducted four-point bending experiments on ZrB_2–SiC ceramic composites at room temperature, observing that the crack growth rate in ceramic materials depends on grain boundary strength and grain size.

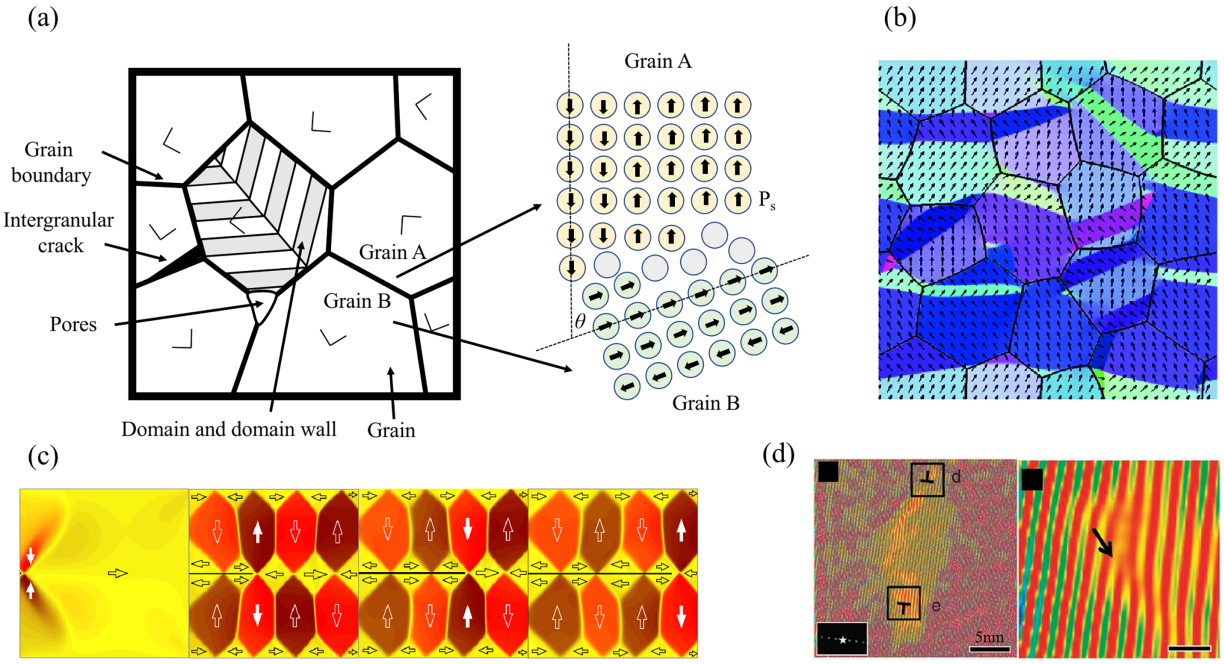

Figure 9: Simulation of the coupling between microstructure and fracture in polycrystalline ferroelectrics. (**a**) Schematic illustrating key microstructural features governing crack paths: grains, grain boundaries, intragranular pores, and a magnified view of ferroelectric domains and domain walls inclined at an angle θ relative to the prospective crack plane. (**b**) Phase field simulation of a polycrystalline ferroelectric ceramic, showing distinct grains separated by boundaries [130]. (**c**) Phase-field simulation snapshots of the evolution of the domain, twins and permeable crack, revealing the interaction between the crack propagation and the formation and evolution of microstructure [131]. (**d**) Domain morphology evolution under dislocation defects via *in situ* TEM. The domain wall can be pinned by the edge dislocation cores pointed by the black arrow [132].

Experimental studies provide fundamental insights into the relationships between grain/grain boundaries and the properties of ferroelectric materials. Nevertheless, they are subject to intrinsic constraints. For instance, experiments struggle to precisely control single variables: variations in grain size are often accompanied by changes in grain boundary structure and other factors, making it difficult to isolate the sole influence of grain size. Moreover, the coupled effects of experimental parameters are complex, and it is challenging to fully capture actual service conditions [133]. These limitations have promoted the application of simulation techniques in this field. Cotterill et al. [134] first employed the Molecular Dynamics (MD) method to study grain boundaries, demonstrating MD's capability to provide atomic-level insights into macroscopic problems. Another approach is the Monte Carlo (MC) method. Unlike Molecular Dynamics (MD), the Monte Carlo (MC) method does not solve equations of motion and thus does not provide a physical trajectory. Instead, it uses random number sequences to propose system configuration changes, which are accepted or rejected to yield correct thermodynamic averages. Srolovitz [135] used MC method to simulate the microstructure of equiaxed grains. However, these simulation methods also have their

own limitations. MD simulations are constrained by limited temporal and spatial scales, preventing crack propagation modeling in macroscopic polycrystalline materials. MC incurs high computational costs and exhibits slow convergence for complex problems.

The PFM has unique advantages for capturing local phenomena and simulating material microstructure. Traditional model often assume sharp phase interfaces and abrupt transitions. In contrast, phase-field simulations overcome the limitations of the sharp-interface concept by treating the phase interface as a transitionally diffuse region [136]. In 1994, Chen and Yang [137] first applied the PFM to simulate grain growth, demonstrating its suitability for grain boundary dynamics simulations in polycrystalline materials. Building on this, Moelans et al. [138] incorporated anisotropy, developing generalized polycrystalline phase-field models for simulating grain growth in anisotropic systems. This model offers highly controllable numerical accuracy, describes arbitrary orientation- and inclination-dependent dependencies grain boundary energy and mobility, and enables 2D/3D simulations of phase transformations and diffusion in polycrystalline, multiphase, and multicomponent structures. Ghiglione et al. [139] combined Cosserat continuum theory with PFM to perform mesoscopic and full-field simulations of recrystallization nucleation stage in plastically deformed single crystals. Zhang and Liu developed a phase field grain growth model to predict the grain distribution in ferroelectric ceramics, though without incorporating domain information [140].

In recent years, phase-field models for polycrystalline materials have been extensively developed, with current research exploring their coupling with other factors, for instance, phase separation [141,142], ferroelectric domain [130,143] (see Fig. 9b), and fracture [144], etc. Given that transgranular and intergranular cracking are the primary fracture modes in ceramics, coupling fracture mechanics with polycrystalline models has become a key research focus for addressing ceramic brittleness, particularly in ferroelectric. Abdollahi and Arias [145] developed a phase-field model simulating crack propagation in ferroelectric anisotropic polycrystalline barium titanate. Their model accounted for the effects of different crystallographic orientations, though all grain boundaries shared identical crack surface and grain boundary energy. Emdadi and Asle Zaeem [144] incorporated elastic anisotropy and grain boundary energy parameters, establishing phase-field frameworks to investigate intergranular and transgranular crack propagation mechanisms in brittle polycrystalline materials. Results show that specific combinations of grain boundary strength and crack surface energy can induce and promote intergranular crack propagation, thereby contributing to fracture toughness.

5.1.2 Domain and Domain Wall

Domain and domain walls are crucial for determining ferroelectric properties, affecting fatigue behavior [146], piezoelectric performance, dielectric feature [147], fracture toughness, crack propagation (see Fig. 9c) and other characteristics [10]. Under mechanical loading, strong stress fields at crack tips induce domain switching (primarily 90° domain switching), forming a domain-switched zone that significantly enhances fracture toughness [148]. Under cyclic electric loading, incompatible 90° domain switching generates interfacial shear stress, driving crack propagation [149]. When propagating cracks encounter pre-existing domain walls, their behavior changes markedly, depending on interaction angles. Recent phase-field simulations and indentation experiments reveal that this interaction exhibits pronounced anisotropy [63].

Researchers have proposed models to explain how domain structures affect ferroelectric properties, based on experimental observations. In early studies, Matthias and Von Hippel [150] first observed domain structures in barium titanate using polarizing microscopy and X-ray diffraction. Forsbergh [151] also observed wedge-shaped lamellar domain structures in single crystals, and investigated configurations and formation rules of various domain types. Nakamura [152] employed the moving wave theory to describe the lateral motion of 180° domain walls in ferroelectric barium titanate. These early studies proposed

several models characterizing domains and domain wall formation and motion; however, these models were purely phenomenological and did not fully clarify underlying mechanisms. With advances in microscopy, subsequent research has deepened understanding of domains and domain wall structures and dynamics, establishing theoretical models [153–155].

In recent years, research on domains and domain walls has advanced significantly. Researchers have begun designing and fabricating domains and domain walls through domain engineering, opening a promising route for ferroelectric device applications. For instance, Li et al. [156] regulated the anchoring forces on ferroelectric liquid crystal molecules using photopatterning, achieving controllable continuous rotation and multidimensional manipulation of spontaneous polarization within fluidic ferroelectric domains. Zahn et al. [157] studied electric field-driven domain wall motion, demonstrating long-range reversible domain wall displacement.

Although classic experiments have revealed the domain and domain-wall structures, they are limited by their spatiotemporal resolution. With the development of computational physics, simulation methods such as MD [158], MC [159], and PFM [160,161] have been applied. Among these, PFM reveals the multiphysical field-coupling mechanism and flexibly describe complex microstructures, making it widely used for simulating domains and domain walls [117]. Chen and Shen [162] first established a fundamental framework for phase-field simulation of ferroelectrics, based on the time-dependent Ginzburg-Landau equations, to calculate the equilibrium states and domain structure evolution. Li et al. [163] developed a phase-field model that predicts detailed domain structures and their temporal evolution during a ferroelectric transition in ferroelectric thin films.

Classical ferroelectric phase-field models, which treat spontaneous polarization or material polarization as a continuous order parameter coupled with electrostatic and elastic energies, have successfully elucidated the microscopic dynamics of domain nucleation and wall migration under external fields. However, this framework typically presupposes mesoscopic material continuity and focuses on polarization evolution, rather than accounting for material damage. This limitation is significant because, in operating ferroelectric devices under combined electromechanical loading, crack initiation and propagation constitute a dominant failure mechanism. The processes of crack evolution and domain/domain wall dynamics are intrinsically coupled; thus, an isolated consideration of the domain structure is insufficient for accurately predicting material failure [164]. This recognition has motivated the integration of fracture mechanics into the phase-field framework to study the coupled evolution of cracks and domains. For instance, Wang and Zhang employed a phase-field model to simulate polarization switching near a crack tip and its effect on fracture toughness [165]. Xu et al. developed a phase-field fracture model incorporating a damage variable to investigate crack behavior and its interaction with domain structures [114]. More recently, Liu et al. [74] established a fully coupled phase-field model that simulates concurrent domain structure evolution and crack propagation, further incorporating the influence of the flexoelectric effect.

5.1.3 Defects

In early research in ferroelectrics, defects were primarily regarded as material imperfection manifestations, and their performance effects were mostly interpreted as negative. Representative studies focused mainly on identifying defect types, observing impacts on macroscopic performance, exploring the interactions between defect and other microstructures(see Fig. 9d), and establishing correlations between defects and performance variations. Kim et al. [166] investigated defect effects in improper ferroelectrics on pyroelectric response. Since ferroelectric ceramics are often subjected to alternating current in practical applications, reliability studies are required [167]. Subsequent studies combined theoretical fatigue models to explore microphysical mechanisms through which defects affect ferroelectric performance. For instance,

Brennan [168] developed a ferroelectric fatigue model based on Landau theory, finding that charged defect and polar domain interactions produce defect activation energies that increase with charge accumulation in defect planes, leading to logarithmic polarization decay with switching cycles. Park and Chadi [169] discussed oxygen vacancy effects on fatigue and polarization in ferroelectric perovskites, identifying oxygen vacancies as potential sources of domain pinning and polarization fatigue in $PbTiO_3$. He and Vanderbilt [11] investigated oxygen vacancy interactions with 180° domain walls in tetragonal $PbTiO_3$ using density-functional theory, confirming defect tendencies to migrate to and pin at domains. These fatigue models describe the progressive damage accumulation induced by defects during cyclic loading [168]. Beyond a critical threshold, such accumulated damage localizes, often through the nucleation, growth, and coalescence of microcracks, ultimately leading to macroscopic crack initiation and fracture [170]. Soh et al. [171] proposed a failure criterion based on the strain energy density factor for the fracture behavior of piezoelectric materials containing elliptical holes or cracks under coupled electromechanical loading, finding that defects affect crack initiation locations and critical loads. Geng and Yang [172,173] proposed a finite element scheme to investigate the motion and coalescence of point defects under the combined action of diffusion on pore surfaces and domain wall migration. However, limited by the simulation scale, this model struggles to track the motion of a large number of pores.

The PFM is particularly well-suited for investigating defect-fracture interactions in ferroelectric materials due to its inherent capability to handle coupled multiphysics and evolving phase interfaces within a unified framework. This allows for the concurrent simulation of complex micro-mechanisms, such as the evolution of defect structures, their interaction with ferroelectric domains, and the resulting crack initiation and propagation. Leveraging this strength, PFM has been effectively applied to quantify how specific defects influence fracture behavior. For instance, Mohanty et al. [174] employed a phase-field model to study brittle fracture in piezoelectric ceramics, with a focus on the role of porosity. Their work demonstrated that the spatial distribution of pores significantly affects the fracture load. Notably, an orderly arrangement of pores was found to enhance the structural reliability more effectively than a single pore or a random distribution, offering valuable insight for the topology optimization of piezoceramic components designed for improved fracture resistance.

5.2 Fracture Model Coupled with Dielectric Breakdown

The investigation of dielectric breakdown in ferroelectric materials, and its critical coupling with mechanical fracture, constitutes a key research frontier for ensuring device reliability. The theoretical foundation for this coupled problem was established through a seminal analogy drawn by Suo [175], who extended the Griffith energy balance framework from fracture mechanics to the electrical domain. This work reconceptualized the propagation of a conductive breakdown channel as being governed by a competition between an electrical energy release rate and a material's "breakdown toughness". It thereby established a theoretical paradigm that dielectric breakdown resistance, akin to fracture toughness, could be enhanced through deliberate microstructural design. Early research in this area was strongly driven by the industrial imperative to develop reliable, high-dielectric-constant materials for integrated circuits.

Early systematic studies on ferroelectric ceramics, such as barium-strontium titanate (BST) for DRAM applications, demonstrated that the dielectric breakdown strength is not an intrinsic material property but is critically influenced by microstructure [176]. Key evidence includes the independence of breakdown field from film thickness and its clear dependence on electrode area, supporting a failure mechanism mediated by defects and conductive pathways within the microstructure, as described by the Gerson-Marshall hypothesis. This established the foundational concept that microstructure dictates the breakdown mechanism. Subsequent research on ferroelectric thin films refined this understanding by introducing a

"charge-to-breakdown" model. This model posits that failure is directly linked to the total charge injected into the film, which drives the accumulation of defects until a percolative conductive path forms [177]. This framework successfully explains the time-dependent nature of breakdown and highlights the decisive roles of electrode interfaces and pre-existing fatigue damage in determining reliability. The generality of the empirical scaling law for breakdown strength, often expressed as

$$E_b(d) = \gamma d^{-\xi} \tag{25}$$

has been validated even under extreme thermodynamic conditions, where d is the thickness of the dielectric thin film, E_b the breakdown electric field, γ and ξ the material and mechanism related constants. Remarkably, this thickness-dependent law holds for ferroelectrics subjected to adiabatic compression, confirming the robustness of the underlying microstructural defect-mediated failure paradigm across vastly different physical states [178].

Theoretical and experimental progress converged to clarify the key material parameters governing breakdown. A comprehensive review [179] systematized the various mechanisms, from intrinsic electronic processes to thermal runaway, emphasizing the unique role of ferroelectric domain dynamics. Controlled experimental studies provided definitive evidence that materials with lower remnant polarization and dielectric constant, such as relaxor ferroelectrics featuring polar nanoregions (PNRs), inherently exhibit superior breakdown strength, a finding critical for high-energy-density applications [180]. This mechanistic understanding was successfully translated into practice through the experimental fabrication of multilayer heterostructures, in which engineered interfaces and barrier layers were shown to redistribute internal electric fields and physically impede breakdown paths, thereby validating the early design principles [181].

Given its unique capability to handle diffuse interfaces and coupled multi-physics, the PFM has become the preeminent tool for quantifying and visualizing the intertwined evolution of ferroelectric domains and dielectric breakdown. Early simulations leveraged PFM to explore the design of composite dielectrics, revealing that the incorporation of metallic particles can dangerously concentrate local electric fields, whereas strategically placed insulating particles can effectively pin and hinder the propagation of conductive "treeing" channels, thereby enhancing the overall dielectric strength [182]. By self-consistently coupling ferroelectric polarization kinetics with a damage order parameter, this model enabled the demonstration that higher domain-switching mobility can significantly increase dielectric breakdown strength by dissipating energy and delaying catastrophic failure [183]. Subsequent phase-field studies have systematically dissected the roles of various microstructural features: the size and location of pores [184], the thickness, permittivity, and associated grain size effects of grain boundaries [185], and the influence of external mechanical stress, which can either promote or suppress breakdown depending on its sign [182]. Furthermore, phase-field modeling serves as a critical bridge to manufacturing by simulating the filling of nanoparticles into polymers, it reveals that the breakdown strength can be tuned by the material parameters of the filler nanoparticles, thereby providing guidance to both theorists and experimentalists in the design of high-energy-density materials and devices (see Fig. 10a).

Future research in this area is poised to address several outstanding challenges. A primary direction is the development of fully integrated phase-field models in which the crack field and the breakdown damage field evolve competitively under coupled electromechanical loading, thereby explicitly predicting the failure mode. Incorporating more detailed, physically based descriptions of charge-injection and defect-generation kinetics into the breakdown criterion will move the models beyond phenomenological energy thresholds.

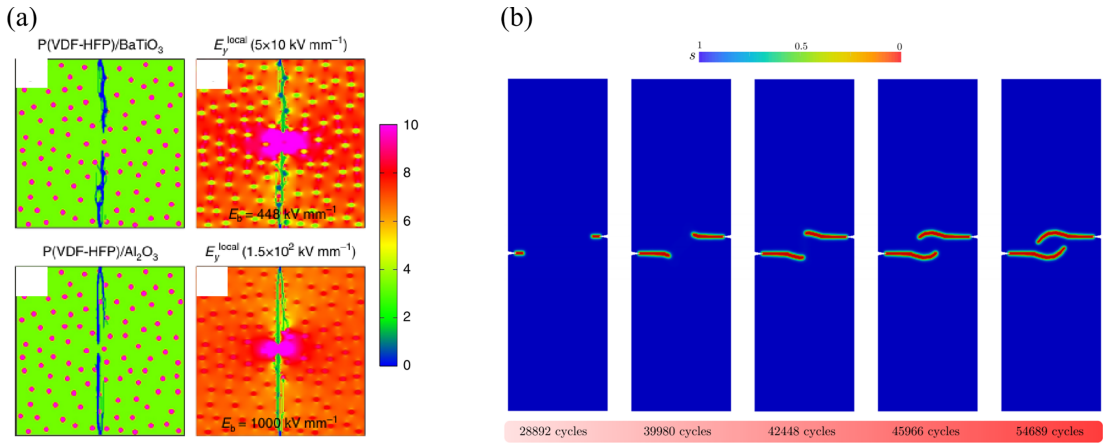

Figure 10: (**a**) Phase field simulation of the breakdown process of composite dielectric materials, highlighting that the breakdown strength of the polymer can be altered by the blending of metallic oxide nanoparticles [186]. (**b**) Simulated evolution of fatigue damage or crack patterns under increasing numbers of loading cycles, highlighting the progressive accumulation of damage [187].

5.3 Fatigue in Ferroelectrics

The reliability of ferroelectric ceramics under cyclic electromechanical loading, often termed fatigue, is a critical concern for their long-term performance in actuators, sensors, and transducers. Fatigue in these materials manifests primarily as a gradual degradation of functional properties and, more critically, as subcritical crack growth leading to catastrophic failure. Research in this field has evolved from pioneering theoretical concepts to sophisticated experimental characterizations and advanced computational modeling, building a multi-scale understanding of the underlying mechanisms.

The foundational theoretical framework for electric-field-driven fatigue crack growth was established by Zhu et al. [188]. They proposed a mechanism where incompatible strains generated by domain switching near a crack tip under an alternating electric field induce local stress concentrations sufficient to drive crack propagation. This concept of domain-switching-induced stress became a key concept for interpreting subsequent experimental observations.

Experimental investigations in the mid-2000s provided robust validation and deeper insights. Fang and colleagues conducted a series of seminal studies. They first systematically demonstrated fatigue crack growth in polycrystalline PZT under purely cyclic electric fields and formulated an empirical Paris law, establishing the crack growth rate (da/dN) as a power-law function of the applied electric field intensity [189]. Employing $BaTiO_3$ single crystals and *in situ* observation, they achieved the first direct visualization of the synchronized process of 90° domain switching and crack advance, revealing a characteristic "jump-like" propagation mode [190]. Concurrently, Salz et al. elucidated the effect of pure mechanical cycling, showing that fatigue crack growth under cyclic mechanical loads occurs independently of the initial poling state, highlighting a distinct mechanical degradation pathway [191].

A significant advancement came from Westram et al., who unified the understanding of fatigue under combined loading [192]. Through rigorous fracture mechanics experiments and analysis, they proposed a universal fatigue crack growth law governed by a single parameter: the electric displacement intensity factor range, ΔK_{IV}. Their work identified crack-closure effects induced by residual depolarization fields as the key mechanism explaining the increased fatigue threshold under combined electromechanical loading compared with pure electrical loading.

In parallel with experimental efforts, theoretical models were developed to provide predictive capabilities. Wang and Han formulated an analytical accumulation damage model by extending the accumulated plastic displacement criterion from metal fatigue to ferroelectrics [193]. Assuming electrical and mechanical saturation zones ahead of the crack tip, they derived a closed-form Paris-type law where da/dN is proportional to the fourth power of an effective stress intensity factor range, ΔK_{eff}, which linearly combines mechanical and electrical loading components. This model theoretically confirmed the Paris law relationship and predicted that an applied electric field could either enhance or suppress crack growth depending on its direction, even suggesting a condition for complete crack arrest.

The subsequent decade was characterized by an increased emphasis on application-oriented and simulation-driven research. A key indicator of this shift was the comprehensive review by Glaum and Hoffman, which synthesized the progress and persistent challenges in lead-free piezoelectric materials, a field of growing application-oriented interest [194]. A comprehensive review by Genenko et al. synthesized mechanisms of aging and fatigue, emphasizing the interplay between domain dynamics and defect chemistry [195]. To address high-cycle fatigue life prediction, Lange and Ricoeur developed a mesoscopic model that accounts for complex electromechanical coupling under cyclic loads, enabling the study of design trade-offs [196]. At the mesoscale, Kozinov and Kuna performed a pioneering numerical simulation by directly coupling a 3D ferroelectric grain-switching model with an electromechanical cyclic cohesive zone model at grain boundaries [197]. Their approach enabled simulation of damage initiation and evolution in a realistic polycrystalline microstructure, revealing different failure modes under purely electrical vs. purely mechanical cycling.

Recent advances in experimental techniques, offering high spatiotemporal resolution, have provided unprecedented detail into fatigue crack growth mechanisms, prompting critical refinements to established theoretical models. A prime example is the work of Li et al. [198], who employed digital image correlation (DIC) coupled with *in situ* observation to capture the fatigue crack growth process in PZT ceramics. Their study yielded two pivotal insights that challenge prior theoretical frameworks. Firstly, they demonstrated that steady-state crack propagation occurs during the phase of electric field reversal and crack closure, rather than during crack opening. Secondly, their observations revealed that a strong incompatible domain-switching zone forms ahead of a blunt notch but is conspicuously absent ahead of a sharp crack tip. These findings indicate that the classic domain-switching-driven fatigue model, which relies on the stress field from such an incompatible zone, may primarily govern the initial crack "pop-in" from a notch. In contrast, the subsequent propagation of a sharp crack likely involves a competition between multiple mechanisms, such as dielectric breakdown-induced bubbling, crack surface wedging, and grain-to-grain interactions, as the authors subsequently discuss.

The study of fatigue in ferroelectrics has evolved from initial phenomenological reports into a multifaceted discipline encompassing mechanistic theory, fracture mechanics-based life prediction, and high-fidelity computational simulation. In recent years, the phase-field model has emerged as a powerful and widely-adopted tool for predicting crack propagation and fatigue life. Schreiber et al. [187] recently using PFM to investigate the evolution of fatigue damage or crack patterns under increasing numbers of loading cycles, highlighting the progressive accumulation of damage.(see Fig. 10b) By naturally bridging micro-scale damage mechanisms with macro-scale failure processes, this cross-scale theoretical framework offers a promising avenue to revitalize the classical discipline of fatigue life prediction, especially through its capability to incorporate complex microstructural evolution, multi-physics coupling, and stochastic effects that are difficult to capture with traditional methods [199–201].

While a universal description based on effective intensity factors has been established for macroscopic crack growth, recent high-resolution experiments highlight the complexity of the underlying micro-mechanisms, particularly for sharp cracks. The gap between microscopic crack initiation and propagation and macroscopic fatigue behavior remains a challenge.

The preceding sections have detailed the PFM's capabilities in modeling distinct failure mechanisms—fracture, dielectric breakdown, and fatigue—often in isolation. However, in operating ferroelectric devices, these mechanisms seldom occur independently. Instead, they interact, compete, and can sequentially trigger one another, defining the ultimate reliability limit. For instance, cyclic fatigue damage can localize to nucleate a dominant crack, which in turn concentrates the electric field and may precipitate dielectric breakdown. Conversely, an evolving breakdown path can alter the local stiffness and stress field, deflecting or accelerating a growing crack. This intrinsic coupling necessitates a modeling paradigm shift from analyzing isolated failures to explicitly simulating their competition.

5.4 Integration of Machine Learning

Machine learning (ML) has emerged as a transformative paradigm in computational materials science, providing powerful strategies to overcome the persistent challenges of prohibitive computational expense and limited exploration of design spaces in the multi-scale modeling, performance prediction, and inverse design of ferroelectric materials. The application of ML in this context follows two principal, complementary strands: data-driven surrogate modeling and physics-informed neural networks (PINN), see Fig. 11.

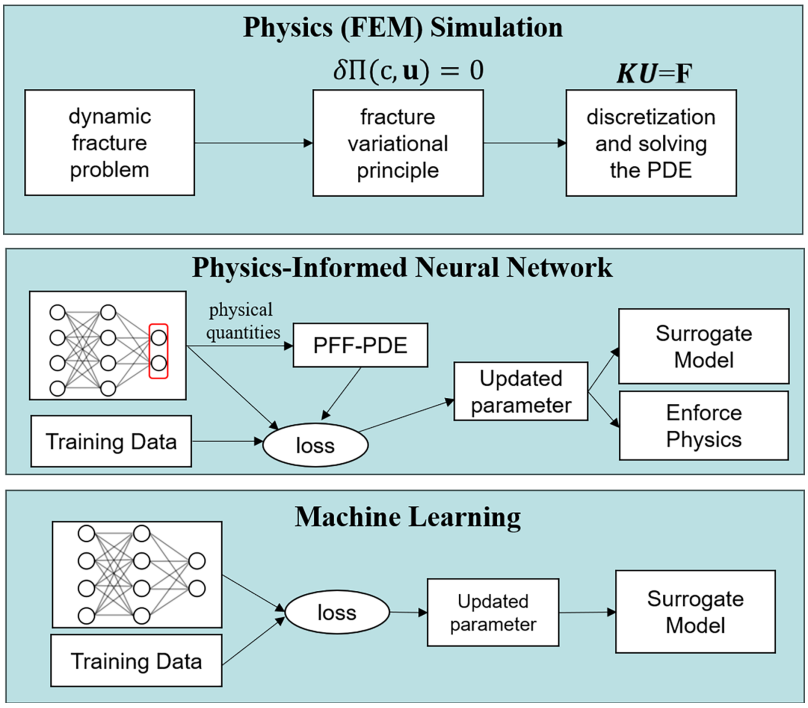

Figure 11: Comparison between different methods for fracture simulation.

ML offers a data-driven pathway to circumvent the computational bottlenecks of high-fidelity simulations. In this approach, ML algorithms are trained to learn the complex, high-dimensional relationships between input parameters (e.g., microstructure, loading conditions) and output fields (e.g., stress, polarization, damage) from datasets generated by first-principles or phase-field calculations. The resulting

surrogate models provide near-instantaneous predictions, effectively emulating the outcome of expensive simulations at a fraction of the computational cost, thereby enabling rapid parametric studies and design space exploration. Early foundational work demonstrated the feasibility of this approach for ferroelectric phase-field modeling. Alhada-Lahbabi et al. developed a dedicated U-Net convolutional neural network (CNN) surrogate that could stably predict the evolution of ferroelectric domains over long time scales from random initial states, achieving remarkable accuracy and an acceleration factor exceeding 685 times for 2D simulations [58] (See Fig. 12b). This work validated the core concept of replacing traditional partial differential equation solvers with data-driven models. The methodology was subsequently advanced to tackle more complex, application-relevant scenarios. Alhada-Lahbabi et al. extended the surrogate framework to three dimensions and, critically, to dynamic electrical boundary conditions mimicking an atomic force microscopy tip, enabling the simulation of tip-induced domain switching with a 2500× speed-up [202]. This level of acceleration is a prerequisite for practical inverse design using techniques such as reinforcement learning. Beyond accelerating single simulations, data-driven ML frameworks have been constructed for higher-level engineering tasks. As shown in Fig. 12c, de Moraes et al. integrated supervised ML classifiers with a damage-fatigue phase-field model to create a data-driven framework for failure prediction and classification, showcasing the potential for real-time structural health monitoring [203].

The second pathway addresses a different scenario, where strict adherence to known physical laws is paramount, or where high-fidelity training data is exceptionally scarce or costly to obtain. In this physics-informed paradigm, governing equations, conservation laws, or thermodynamic principles are directly embedded into the ML architecture or its training objective, ensuring that predictions remain consistent with the underlying physics. A prominent example is the use of PINNs. Shang et al. introduced an "en-PF PINN" that incorporates the energy dissipation law as a constraint, allowing it to directly predict the steady-state ferroelectric microstructure without simulating the costly transient evolution [204]. In a related work, Konale and Srivastava demonstrated that PINNs can be used as a mesh-free solver for fracture mechanics problems, offering a novel framework that avoids the need for gradient-based damage regularization [205] (See Fig. 12a).

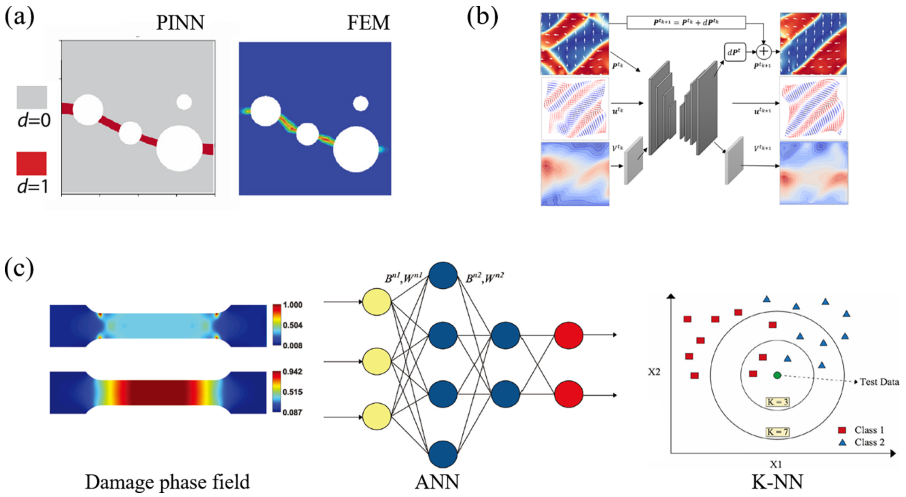

Figure 12: Three ML paradigms applied to PFM. (**a**) A PINN provides accelerated prediction of the crack phase-field compared to traditional FEM simulation [205]. (**b**) A CNN-based surrogate model learns the direct mapping from input microstructural/loading parameters to the output steady-state ferroelectric domain structure [58]. (**c**) Supervised learning models are trained on damage phase-field data to classify the global failure state of a specimen [203].

Table 1: Summary of modeling strategies for fracture in ferroelectric materials, highlighting typical application regimes, principal advantages, and key limitations.

Modeling Strategy	Typical Application Regime	Principal Advantages	Key Limitations
Fully Coupled Ferroelectric–Fracture Phase-Field Models	Prediction of crack initiation and propagation in unpoled or domain-evolving materials; analysis of competing failure mechanisms (e.g., fracture vs. dielectric breakdown); investigation of nanoscale phenomena involving strain-gradient (flexoelectric) effects.	Provides a thermodynamically consistent and fully coupled description of crack evolution and polarization dynamics; enables the capture of complex interactions, including domain switching, crack deflection, and multi-mode failure transitions.	High computational cost, particularly in three-dimensional and polycrystalline settings; requires calibration of multiple material parameters governing coupled electromechanical and fracture responses.
Sequentially Coupled or Degradation-Based Approaches	Simulation of fatigue crack growth with cycle-dependent damage accumulation; analysis of fracture in pre-poled materials with relatively stable domain configurations.	Reduced computational complexity compared to fully coupled formulations; facilitates incorporation of phenomenological or experimentally calibrated degradation laws.	Does not fully resolve the strong coupling between crack propagation and domain evolution; limited predictive capability for crack initiation and transient electromechanical interactions.
Linear Piezoelectric Fracture Mechanics	Evaluation of fracture behavior in poled, coarse-grained ceramics under small electric fields and limited domain switching; use in preliminary design assessments and parametric studies.	Availability of analytical or semi-analytical solutions; well-established framework for the evaluation of electromechanical stress intensity factors.	Restricted to linear constitutive behavior and thus unable to capture nonlinear domain switching, crack branching, or microstructural effects; limited validity under strong electric loading conditions where nonlinear electromechanical coupling dominates.

The synergy between data-driven surrogate models and physics-informed learning is forging a new, intelligent toolkit for ferroelectric materials research. From discovering atomic-scale mechanisms with machine learning interatomic potentials (MLIPs) to accelerating mesoscale design with CNN surrogates, and from predicting engineering failure to enabling inverse design, these ML-powered approaches are closing the loop on a comprehensive, efficient, and intelligent materials development platform.

6 Conclusion and Future Work

The PFM has firmly established itself as the preeminent computational framework for modeling fracture in ferroelectric materials. Its principal strength lies in a unified variational formulation that naturally couples the evolution of a diffuse crack with the complex, nonlinear evolution of polarization domains and other microstructural elements. As reviewed, this capability has enabled significant advances in understanding and predicting how grain boundaries, domain switching, and defects influence crack paths and toughness; how flexoelectric effects modulate behavior at small scales; how dielectric breakdown competes with mechanical fracture; and how damage accumulates under fatigue loading. The integration of ML promises to further revolutionize the field by drastically reducing computational cost for parametric studies and enabling novel solver strategies.

Despite considerable progress, several key challenges and opportunities for future research persist:

Fully Coupled Multiphysics Models: Developing robust phase-field models that fully couple crack propagation with other concurrent failure modes, such as dielectric breakdown or fatigue microdamage, remains a challenge. Future models should self-consistently predict whether a structure fails due to mechanical crack propagation, electrical breakdown, or their interaction.

Refined Physical Mechanisms: Incorporating more detailed, physics-based descriptions of underlying micromechanisms is crucial. This includes explicit modeling of charged defects (e.g., oxygen vacancies) and their dynamics, as well as their interactions with domain walls and crack tips, as well as refined electrical boundary conditions for evolving crack surfaces that account for local breakdown and conduction.

Bridging Scales: A concerted effort is needed to strengthen the links between phase-field simulations at the mesoscale and both atomistic insights (from machine learning potentials) and macroscopic, quantitative experimental validation. Developing standardized benchmarks and directly comparing simulated crack paths, R-curves, and fatigue lives with high-resolution experiments will be essential for improving predictive credibility.

Focus on Lead-Free and Advanced Materials: The framework must be increasingly applied to and validated for environmentally friendly lead-free ferroelectrics and emerging material systems (e.g., HfO_2-based films), whose fatigue and fracture mechanisms may differ from traditional PZT.

Path to Engineering Design: Ultimately, the goal is to transition phase-field models from tools for mechanistic understanding to components of a holistic materials-by-design workflow. This involves tighter integration with machine learning to enable inverse design of fracture-resistant microstructures and to link simulation outcomes to component-level reliability assessments for specific applications.

To translate phase-field models from research tools to components of a design workflow, clear guidance on their application is needed. The choice of modeling fidelity—from fully coupled ferroelectric-fracture PFM to simplified approaches—should be driven by the specific failure mechanism, material system, and design question. Table 1 provides a concise decision framework. A fully coupled PFM is essential when investigating the competitionor synergy between different failure modes (e.g., crack deflection driven by domain switching, or the transition from dielectric degradation to mechanical crack propagation). For problems where the failure mode is predetermined and dominated by a single physics (e.g., fatigue crack growth in a stable domain structure), a sequentially or weakly coupled approach may be sufficient and far more computationally efficient.

The primary bottlenecks for applying these models to industrial-scale design remain the prohibitive computational cost of 3D, polycrystalline, fully-coupled simulations and the challenge of parameter calibration and validation across material batches and scales. Future efforts must therefore focus on the tighter integration of machine learning for the development of accurate surrogate models and for inverse design of fracture-resistant microstructures. Furthermore, establishing robust protocols to link PFM predictions of microstructure-sensitive crack initiation to component-level probabilistic reliability assessments is crucial. Addressing these challenges will require close collaboration between mechanician, experimentalists, and engineers. By providing both fundamental understanding and practical guidelines, the PFM can fully realize its potential as a predictive design tool, accelerating the development of reliable, high-performance ferroelectric devices.

Acknowledgement: Shuai Wang acknowledges support from the National Natural Science Foundation of China under grant No. 12402182. Min Yi acknowledges the Outstanding Youth Fund of Jiangsu Province (BK20240077). This work is partially supported by High Performance Computing Platform of Nanjing University of Aeronautics and Astronautics.

Funding Statement: National Natural Science Foundation of China 12302182. Outstanding Youth Fund of Jiangsu Province BK20240077.

Author Contributions: The authors confirm contribution to the paper as follows: conceptualization, Shuai Wang and Min Yi; writing (original draft preparation): Shuai Wang and Ke Han; literature collection and analysis: Ke Han; writing

(review and editing): Shuai Wang and Min Yi; supervision: Shuai Wang and Min Yi; funding acquisition: Shuai Wang and Min Yi. All authors reviewed and approved the final version of the manuscript.

Availability of Data and Materials: Not applicable.

Ethics Approval: Not applicable.

Conflicts of Interest: The authors declare no conflicts of interest.

References

1. Scott JF. Applications of modern ferroelectrics. Science. 2007;315(5814):954–9. doi:10.1126/science.1129564.
2. Kuna M. Fracture mechanics of piezoelectric materials—where are we right now? Eng Fract Mech. 2010;77(2):309–26. doi:10.1016/j.engfracmech.2009.03.016.
3. Zhang F, Li W, Yang J, Gao X, Chen L, Qu Z. Theoretical models of the electric field dependent mode i fracture toughness and fracture strength for ferroelectric ceramics. Theor Appl Fract Mech. 2025;139(6):105073. doi:10.1016/j.tafmec.2025.105073.
4. Webber KG, Vögler M, Khansur NH, Kaeswurm B, Daniels JE, Schader FH. Review of the mechanical and fracture behavior of perovskite lead-free ferroelectrics for actuator applications. Smart Mater Struct. 2017;26(6):063001. doi:10.1088/1361-665x/aa590c.
5. Schrade D, Müller R, Xu BX, Gross D. Domain evolution in ferroelectric materials: a continuum phase field model and finite element implementation. Comput Method Appl M. 2007;196(41–44):4365–74.
6. Hao T-H, Shen Z-Y. A new electric boundary condition of electric fracture mechanics and its applications. Eng Fract Mech. 1994;47(6):793–802. doi:10.1016/0013-7944(94)90059-0.
7. Li Y, Chen Z, Wang X, Wang J. Electrical boundary condition at the crack surface in ferroelectrics. J Am Ceram Soc. 2022;105(8):5025–31. doi:10.1111/jace.18469.
8. Pohanka RC, Freiman SW, Bender BA. Effect of the phase transformation on the fracture behavior of $BaTiO_3$. J Am Ceram Soc. 1978;61(1–2):72–5. doi:10.1111/j.1151-2916.1978.tb09234.x.
9. Meschke F, Kolleck A, Schneider GA. R-curve behaviour of $BaTiO_3$ due to stress-induced ferroelastic domain switching. J Eur Ceram Soc. 1997;17(9):1143–9. doi:10.1016/s0955-2219(96)00211-7.
10. Zhu T, Yang W. Fatigue crack growth in ferroelectrics driven by cyclic electric loading. J Mech Phys Solids. 1998;47(1):81–97. doi:10.1016/s0022-5096(98)00082-9.
11. He L, Vanderbilt D. First-principles study of oxygen-vacancy pinning of domain walls in $PbTiO_3$. Phys Rev B. 2003;68(13):134103. doi:10.1103/physrevb.68.134103.
12. Xu Y, Wan W, Dunne PPE. Microstructural fracture mechanics: stored energy density at fatigue cracks. J Mech Phys Solids. 2021;146:104209. doi:10.1016/j.jmps.2020.104209.
13. Suo Z, Kuo C-M, Barnett DM, Willis JR. Fracture mechanics for piezoelectric ceramics. J Mech Phys Solids. 1992;40(4):739–65. doi:10.1016/0022-5096(92)90002-j.
14. Eugene Pak Y. Crack extension force in a piezoelectric material. J Appl Mech. 1990;57(3):647–53.
15. McMeeking RM. Crack tip energy release rate for a piezoelectric compact tension specimen. Eng Fract Mech. 1999;64(2):217–44. doi:10.1016/s0013-7944(99)00068-5.
16. Cao H, Evans AG. Electric-field-induced fatigue crack growth in piezoelectrics. J Am Ceram Soc. 1994;77(7):1783–6. doi:10.1111/j.1151-2916.1994.tb07051.x.
17. Cheng J, Wang B, Du S. A statistical model for predicting effective electroelastic properties of polycrystalline ferroelectric ceramics with aligned defects. Int J Solids Struct. 2000;37(35):4763–81. doi:10.1016/s0020-7683(99)00179-1.
18. Aliabadi MH. Boundary element formulations in fracture mechanics. Appl Mech Rev. 1997;50(2):83–96. doi:10.1115/1.3101690.
19. Cervera M, Barbat GB, Chiumenti M, Wu J-Y. A comparative review of xfem, mixed fem and phase-field models for quasi-brittle cracking. Arch Comput Methods Eng. 2022;29(2):1009–83. doi:10.1007/s11831-021-09604-8.

20. Kiran R, Nguyen-Thanh N, Zhou K. Adaptive isogeometric analysis-based phase-field modeling of brittle electromechanical fracture in piezoceramics. Eng Fract Mech. 2022;274:108738. doi:10.1016/j.engfracmech.2022.108738.
21. Lynch CS. Fracture of ferroelectric and relaxor electro-ceramics: influence of electric field. Acta Mater. 1998;46(2):599–608. doi:10.1016/s1359-6454(97)00225-5.
22. Zhang T-Y, Gao CF. Fracture behaviors of piezoelectric materials. Theor Appl Fract Mech. 2004;41(1–3):339–79. doi:10.1016/j.tafmec.2003.11.019.
23. Bermejo R, Deluca M. Mechanical characterization of PZT ceramics for multilayer piezoelectric actuators. J Ceram Sci Tech. 2012;4(3):159–68.
24. Kondo S, Ishihara A, Tochigi E, Shibata N, Ikuhara Y. Direct observation of atomic-scale fracture path within ceramic grain boundary core. Nat Commun. 2019;10(1):2112. doi:10.1038/s41467-019-10183-3.
25. Zhu DP. Study on domain switching and fracture behavior of ferroelectric single crystals [Ph.D. thesis]. Wuhan, China: Wuhan University; 2021. (In Chinese). doi:10.27379/d.cnki.gwhdu.2021.003242.
26. Cordero-Edwards K, Kianirad H, Canalias C, Sort J, Catalan G. Flexoelectric fracture-ratchet effect in ferroelectrics. Phys Rev Lett. 2019;122(13):135502. doi:10.1103/PhysRevLett.122.135502.
27. Xu M, Tian X, Deng Q, Li Q, Shen S. Directly observing the evolution of flexoelectricity at the tip of nanocracks. Nano Lett. 2022;23(1):66–72. doi:10.1021/acs.nanolett.2c03614.
28. Fang D, Liu J. Fracture mechanics of piezoelectric and ferroelectric solids. Berlin/Heidelberg, Germany: Springer; 2013. 416 p.
29. Qin QH. Fracture mechanics of piezoelectric materials. Southampton, UK: WIT Press.
30. Parton VZ. Fracture mechanics of piezoelectric materials. Acta Astronaut. 1976;3(9–10):671–83. doi:10.1016/0094-5765(76)90105-3.
31. Irwin GR. Analysis of stresses and strains near the end of a crack traversing a plate. J Appl Mech. 1957;24(3):361–4. doi:10.1115/1.4011547.
32. Heyer V, Schneider GA, Balke H, Drescher J, Bahr HA. A fracture criterion for conducting cracks in homogeneously poled piezoelectric PZT-PIC 151 ceramics. Acta Mater. 1998;46(18):6615–22. doi:10.1016/s1359-6454(98)00272-9.
33. McMeeking RM. Towards a fracture mechanics for brittle piezoelectric and dielectric materials. Int J Fract. 2001;108(1):25–41. doi:10.1023/a:1007652001977.
34. Parton VZ, Kudryavtsev BA. Electromagnetoelasticity: piezoelectrics and electrically conductive solids. New York, NY, USA: Gordon & Breach Science; 1988. 503 p.
35. Ricoeur A, Enderlein M, Kuna M. Calculation of the j-integral for limited permeable cracks in piezoelectrics. Arch Appl Mech. 2005;74(8):536–49. doi:10.1007/s00419-004-0370-5.
36. Ou ZC, Chen Y-H. Re-examination of the pkhs crack model in piezoelectric materials. Eur J Mech A/Solids. 2007;26(4):659–75. doi:10.1016/j.euromechsol.2006.09.007.
37. McMeeking RM. The energy release rate for a griffith crack in a piezoelectric material. Eng Fract Mech. 2004;71(7–8):1149–63. doi:10.1016/s0013-7944(03)00135-8.
38. Landis CM. Energetically consistent boundary conditions for electromechanical fracture. Int J Solids Struct. 2004;41(22–23):6291–315. doi:10.1016/j.ijsolstr.2004.05.062.
39. Guo X, Song Z. Physics-informed neural networks for linear elastic fracture mechanics: application of assessing stress intensity factor and transverse stress. Eng Appl Artif Intell. 2025;159:111699. doi:10.1016/j.engappai.2025.111699.
40. Ru CQ. Electric-field induced crack closure in linear piezoelectric media. Acta Mater. 1999;47(18):4683–93. doi:10.1016/s1359-6454(99)00310-9.
41. Tobin AG, Pak E. Effect of electric fields on fracture behavior of PZT ceramics. In: Smart structures and materials 1993: smart materials. Vol. 1916. Washington, DC, USA: SPIE; 1993. p. 78–86.
42. Sun C-T, Park S. Determination of fracture toughness of piezoceramics under the influence of electric field using vickers indentation. In: Smart structures and materials 1995: smart materials. Vol. 2441. Washington, DC, USA: SPIE; 1993. p. 213–22.

43. Kolleck A, Schneider GA, Meschke FA. R-curve behavior of $BaTiO_3$- and PZT ceramics under the influence of an electric field applied parallel to the crack front. Acta Mater. 2000;48(16):4099–113. doi:10.1016/s1359-6454(00)00198-1.
44. Oates WS, Lynch CS, Lupascu DC, Njiwa ABK, Aulbach E, Rödel J. Subcritical crack growth in lead zirconate titanate. J Amer Ceram Soc. 2004;87:1362–4.
45. Zhang Z, Yang B, Gu W, Yu H, Yang L, Shang X, et al. Significantly toughened PZT-based piezoelectric ceramics simultaneously keeping excellent electrical properties via incorporating trace amount of yttria-partially-stabilized zirconia. Ceram Int. 2022;48(23):35614–20. doi:10.1016/j.ceramint.2022.08.299.
46. Mendoza I, Drury D, Koumlis S, Ivy J, Brennecka G, Lamberson L. Combined electromechanical dynamic fracture behavior of lead zirconate titanate (pzt). J Am Ceram Soc. 2022;105(5):3116–22. doi:10.1111/jace.18279.
47. Cui J, Guan K, Rao P, Gong Z, Yu S, Zeng Q, et al. Influence of grain-scale microstructural parameters on fracture toughness of polycrystalline ceramics: dual scale finite element method. J Am Ceram Soc. 2024;107(4):2573–92. doi:10.1111/jace.19598.
48. Mao GZ, Fang DN. Fatigue crack growth induced by domain switching under electromechanical load in ferroelectrics. Theor Appl Fract Mech. 2004;41(1–3):115–23. doi:10.1016/j.tafmec.2003.11.009.
49. Chen PJ. Effects of domain structure on electrically excitable mechanical resonances in ferroelectric ceramics. Int J Solids Struct. 1984;20(2):121–8. doi:10.1016/0020-7683(84)90003-9.
50. Streich FA, Martin A, Webber KG, Kamlah M. Macroscopic constitutive model for ergodic and non-ergodic lead-free relaxors. J Intell Mater Syst Struct. 2022;33(8):1002–17. doi:10.1177/1045389X2110386.
51. Huber JE, Fleck NA. Ferroelectric switching: a micromechanics model versus measured behaviour. Eur J Mech A/Solids. 2004;23(2):203–17. doi:10.1016/j.euromechsol.2003.11.006.
52. Kozinov S, Kuna M. Configurational forces in ferroelectric structures analyzed by a macromechanical switching model. Acta Mech. 2023;234(1):17–36. doi:10.1007/s00707-022-03265-9.
53. Kamlah MJCM. Ferroelectric and ferroelastic piezoceramics—modeling of electromechanical hysteresis phenomena. Contin Mech Thermodyn. 2001;13(4):219–68. doi:10.1007/s001610100052.
54. Schröder J, Romanowski H. A thermodynamically consistent mesoscopic model for transversely isotropic ferroelectric ceramics in a coordinate-invariant setting. Arch Appl Mech. 2005;74(11):863–77. doi:10.1007/s00419-005-0412-7.
55. Miehe C, Rosato D. A rate-dependent incremental variational formulation of ferroelectricity. Int J Eng Sci. 2011;49(6):466–96. doi:10.1016/j.ijengsci.2010.11.003.
56. Pechstein AS, Meindlhumer M, Humer A. High-order mixed finite elements for an energy-based model of the polarization process in ferroelectric materials. J Intell Mater Syst Struct. 2021;32(3):355–68. doi:10.1177/1045389x20953895.
57. Chen L-Q. Phase-field method of phase transitions/domain structures in ferroelectric thin films: a review. J Am Ceram Soc. 2008;91(6):1835–44.
58. Alhada-Lahbabi K, Deleruyelle D, Gautier B. Machine learning surrogate model for acceleration of ferroelectric phase-field modeling. ACS Appl Electron Mater. 2023;5(7):3894–907. doi:10.1021/acsaelm.3c00601.
59. Kreher WS. Influence of domain switching zones on the fracture toughness of ferroelectrics. J Mech Phys Solids. 2002;50(5):1029–50. doi:10.1016/s0022-5096(01)00110-7.
60. Yang W, Fang F, Tao M. Critical role of domain switching on the fracture toughness of poled ferroelectrics. Int J Solids Struct. 2001;38(10–13):2203–11. doi:10.1016/s0020-7683(00)00162-1.
61. Sheng J, Landis CM. Toughening due to domain switching in single crystal ferroelectric materials. Int J Fracte. 2007;143(2):161–75. doi:10.1007/s10704-007-9056-7.
62. Zhang Y, Li J, Fang D. Fracture analysis of ferroelectric single crystals: domain switching near crack tip and electric field induced crack propagation. J Mech Phys Solids. 2013;61(1):114–30.
63. Tan D, Zhuo F, Tian X, Fan H, Wang Q, Zhou X. Anisotropic crack-domain wall interactions in ferroelectric single crystals. Scr Mater. 2026;271(16):117038. doi:10.1016/j.scriptamat.2025.117038.
64. Wang Z, Ricoeur A. Prediction of crack paths in ferroelectrics with anisotropic fracture toughness. Theor Appl Fract Mech. 2021;114(5814):103031. doi:10.1016/j.tafmec.2021.103031.

65. Huber JE, Hofmann F, Barhli S, Marrow TJ, Hildersley C. Observation of crack growth in a polycrystalline ferroelectric by synchrotron X-ray diffraction. Scr Mater. 2017;140:23–6. doi:10.1016/j.scriptamat.2017.06.053.
66. Glazounov AE, Kungl H, Reszat J-T, Hoffmann MJ, Kolleck A, Schneider GA. Contribution from ferroelastic domain switching detected using X-ray diffraction to r-curves in lead zirconate titanate ceramics. J Am Ceram Soc. 2001;84(12):2921–9. doi:10.1111/j.1151-2916.2001.tb01116.x.
67. Kathavate VS, Sonagara H, Praveen Kumar B, Singh I, Eswar Prasad K. Direct observations of changes in ferroelectric domain configurations around the indentation and ahead of the crack front in soft-doped PZT. Materialia. 2021;19(4):101191. doi:10.1016/j.mtla.2021.101191.
68. Schneider GA, Felten F, Mc Meeking RM. The electrical potential difference across cracks in PZT measured by kelvin probe microscopy and the implications for fracture. Acta Mater. 2003;51(8):2235–41. doi:10.1016/S1359-6454(03)00027-2.
69. Xia Y, Qian W, Yang Y. Advancements and prospects of flexoelectricity. ACS Appl Mater Interfaces. 2024;16(8):9597–613. doi:10.1021/acsami.3c16727.
70. Abdollahi A, Peco C, Millán D, Arroyo M, Catalan G, Arias I. Fracture toughening and toughness asymmetry induced by flexoelectricity. Phys Rev B. 2015;92(9):094101. doi:10.1103/physrevb.92.094101.
71. Guo Y, Liu C, Li X. Asymmetric fracture behavior in ferroelectric materials induced by flexoelectric effect. J Appl Phys. 2023;134(24):244102. doi:10.1063/5.0178866.
72. Wang H, Jiang X, Wang Y, Stark RW, van Aken PA, Mannhart J, et al. Direct observation of huge flexoelectric polarization around crack tips. Nano Lett. 2019;20(1):88–94. doi:10.1021/acs.nanolett.9b03176.
73. Zhao X, Soh AK. The effect of flexoelectricity on domain switching in the vicinity of a crack in ferroelectrics. J Eur Ceram Soc. 2018;38(4):1341–8. doi:10.1016/j.jeurceramsoc.2017.10.009.
74. Liu C, Tan Y, Zhang Y, Liu Z, Shimada T, Li X, et al. Phase-field analysis for brittle fracture in ferroelectric materials with flexoelectric effect. Comput Methods Appl Mech Eng. 2024;430(2):117242. doi:10.1016/j.cma.2024.117242.
75. Qi C, Jiang Y, Wang X. Flexoelectric influence on crack propagation in ferroelectric single crystals: a phase-field approach. Smart Mater Struct. 2024;33(8):085051. doi:10.1088/1361-665x/ad65aa.
76. Liu C, Wang C, Li X. Flexoelectric induced crack deflection in $PbTiO_3/SrTiO_3$ superlattices. J Appl Phys. 2025;138(21):215101. doi:10.1063/5.0303246.
77. Pham-Phu T, Kozinov S. Strain gradient enhanced phase-field model for ferroelectric domain evolution. Comput Methods Appl Mech Eng. 2026;451(4):118671. doi:10.2139/ssrn.5409064.
78. Wang S, Su H, Yi M, Shao L-H. Strain gradient finite element formulation of flexoelectricity in ferroelectric material based on phase-field method. Acta Mech Solida Sin. 2024;37(4):570–9. doi:10.1007/s10338-024-00485-5.
79. Linke M, Lammering R. On the calibration of the cohesive strength for cohesive zone models in finite element analyses. Theor Appl Fract Mech. 2023;124:103733. doi:10.21203/rs.3.rs-2288124/v2.
80. Roth S, Hütter G, Kuna M. Simulation of fatigue crack growth with a cyclic cohesive zone model. Int J Fract. 2014;188(1):23–45. doi:10.1007/s10704-014-9942-8.
81. Padilla-Llano DA, Schafer BW, Hajjar JF. Cyclic fracture simulation through element deletion in structural steel systems. J Constr Steel Res. 2022;189(1):107082. doi:10.1016/j.jcsr.2021.107082.
82. Rege K, Lemu HG. A review of fatigue crack propagation modelling techniques using fem and XFEM. In: IOP Conference Series: Materials Science and Engineering. Bristol, UK: IOP Publishing; 2017. Vol. 276.
83. Wu J-Y. Unified analysis of phase-field models for cohesive fracture. Int J Damage Mech. 2024:10567895261429154. doi:10.1177/10567895261429154.
84. Ricoeur A, Kuna M. A micromechanical model for the fracture process zone in ferroelectrics. Comput Mater Sci. 2003;27(3):235–49. doi:10.1016/s0927-0256(02)00360-9.
85. Kozinov S, Kuna M, Roth S. A cohesive zone model for the electromechanical damage of piezoelectric/ferroelectric materials. Smart Mater Struct. 2014;23(5):055024. doi:10.1088/0964-1726/23/5/055024.
86. Kozinov S, Kuna M. Simulation of damage in ferroelectric actuators by means of cohesive zone model. Sens Actuators A Phys. 2015;233(2):176–83. doi:10.1016/j.sna.2015.06.030.

87. Hachi BE, Boudouh M, Ramtani S, Haboussi M, Liu H. Enhanced brittle fracture modeling in heterogeneous materials: a variational phase field approach integrating XFEM and level-set methods. Int J Comput Methods. 2025;22(7):2550003. doi:10.1142/S0219876225500033.
88. Chama M, Moulai-Khatir D, Hamza B, Slamene A, Mokhtari M. Advanced damage prediction in notched plates reinforced with graded composite patches: integrating XFEM-CZM and fiber-matrix coupling laws using functionally graded materials. Mech Adv Mater Struct. 2025;32(13):2998–3015.
89. Vellwock AE, Libonati F. XFEM for composites, biological, and bioinspired materials: a review. Materials. 2024;17(3):745. doi:10.3390/ma17030745.
90. Lee C, Singh IV, Natarajan S. A cell-based smoothed finite-element method for gradient elasticity. Eng Comput. 2023;39(1):925–42. doi:10.1007/s00366-022-01734-2.
91. Wen C, Yan Z, Feng W. The dynamic fracture analyses of an internal crack in piezoelectric plates by XFEM. In: Proceedings of the 2025 19th Symposium on Piezoelectricity, Acoustic Waves, and Device Applications (SPAWDA); 2025 Jul 21–24; Shihezhi, China. p. 276–80.
92. Kumar R, Pathak H, Singh A, Tiwari M. Modeling of crack repair using piezoelectric material: xfem approach. Eng Comput. 2021;38(2):586–617. doi:10.1108/ec-01-2020-0001.
93. Nanthakumar SS, Lahmer T, Rabczuk T. Detection of multiple flaws in piezoelectric structures using XFEM and level sets. Comput Methods Appl Mech Eng. 2014;275(12):98–112. doi:10.1002/nme.5189.
94. Griffith AA. VI. The phenomena of rupture and flow in solids. Philos Trans R Soc Lond Ser A Contain Pap A Math Or Phys Character. 1921;221(582–593):163–98. doi:10.1098/rsta.1921.0006.
95. Francfort GA, Marigo J-J. Revisiting brittle fracture as an energy minimization problem. J Mech Phys Solids. 1998;46(8):1319–42. doi:10.1016/s0022-5096(98)00034-9.
96. Miehe C, Welschinger F, Hofacker M. Thermodynamically consistent phase-field models of fracture: variational principles and multi-field FE implementations. Int J Numer Methods Eng. 2010;83(10):1273–311.
97. Amor H, Marigo J-J, Maurini C. Regularized formulation of the variational brittle fracture with unilateral contact: numerical experiments. J Mech Phys Solids. 2009;57(8):1209–29.
98. Miehe C, Welschinger F, Hofacker M. A phase field model of electromechanical fracture. J Mech Phys Solids. 2010;58(10):1716–40. doi:10.1016/j.jmps.2010.06.013.
99. Hai L, Wriggers P, Huang Y, Zhang H, Xu S. Dynamic fracture investigation of concrete by a rate-dependent explicit phase field model integrating viscoelasticity and micro-viscosity. Comput Methods Appl Mech Eng. 2024;418(7):116540. doi:10.1016/j.cma.2023.116540.
100. Pranavi D, Rajagopal A, Reddy JN. Phase field modeling of anisotropic fracture. Contin Mech Thermodyn. 2024;36(5):1267–82. doi:10.1007/s00161-023-01260-6.
101. Zhang S, Jiang W, Tonks MR. A new phase field fracture model for brittle materials that accounts for elastic anisotropy. Comput Methods Appl Mech Eng. 2020;358(2):112643. doi:10.1016/j.cma.2019.112643.
102. Chen L, Li B, de Borst R. Adaptive isogeometric analysis for phase-field modeling of anisotropic brittle fracture. Int J Numer Methods Eng. 2020;121(20):4630–48. doi:10.1002/nme.6457.
103. Lammen H, Conti S, Mosler J. A finite deformation phase field model suitable for cohesive fracture. J Mech Phys Solids. 2023;178(7):105349. doi:10.1016/j.jmps.2023.105349.
104. Huber W, Zaeem MA. A mixed mode phase-field model of ductile fracture. J Mech Phys Solids. 2023;171(4):105123. doi:10.1016/j.jmps.2022.105123.
105. Behera AK, Unnikrishna Pillai A, Rahaman MM. A phase-field model for electro-mechanical fracture with an open-source implementation of it using gridap in julia. Math Mech Solids. 2023;28(8):1877–908. doi:10.1177/10812865221133860.
106. Luege M, Orlando A. A variational anisotropic phase-field model of quasi-brittle fracture: energetic solutions and their computation. arXiv:2009.05888. 2020.
107. Kuhn C, Schlüter A, Müller R. On degradation functions in phase field fracture models. Comput Mater Sci. 2015;108(4):374–84. doi:10.1016/j.commatsci.2015.05.034.
108. Pham KH, Ravi-Chandar K, Landis CM. Experimental validation of a phase-field model for fracture. Int J Fract. 2017;205(1):83–101. doi:10.1007/s10704-017-0185-3.

109. Chen L-Q. Phase-field models for microstructure evolution. Annu Rev Mater Res. 2002;32(1):113–40. doi:10.1146/annurev.matsci.32.112001.132041.
110. Kobayashi R. Modeling and numerical simulations of dendritic crystal growth. Phys D Nonlinear Phenom. 1993;63(3–4):410–23. doi:10.1016/0167-2789(93)90120-p.
111. Carl E, Krill III, Chen L-Q. Computer simulation of 3-D grain growth using a phase-field model. Acta Mater. 2002;50(12):3059–75. doi:10.1016/s1359-6454(02)00084-8.
112. Wang J, Shi S-Q, Chen L-Q, Li Y, Zhang T-Y. Phase-field simulations of ferroelectric/ferroelastic polarization switching. Acta Mater. 2004;52(3):749–64. doi:10.1016/j.actamat.2003.10.011.
113. Zhang JX, Chen LQ. Phase-field model for ferromagnetic shape-memory alloys. Philos Mag Lett. 2005;85(10):533–41. doi:10.1080/09500830500385527.
114. Xu B-X, Schrade D, Gross D, Mueller R. Fracture simulation of ferroelectrics based on the phase field continuum and a damage variable. Int J Fract. 2010;166(1):163–72.
115. Schrade D, Müller R, Gross D. On the physical interpretation of material parameters in phase field models for ferroelectrics. Arch Appl Mech. 2013;83(10):1393–413. doi:10.1007/s00419-013-0754-5.
116. Marton P, Rychetsky I, Hlinka J. Domain walls of ferroelectric $BaTiO_3$ within the ginzburg-landau-devonshire phenomenological model. Phys Rev B Condens Matter Mater Phys. 2010;81(14):144125. doi:10.1103/PhysRevB.81.144125.
117. Wang J-J, Wang B, Chen L-Q. Understanding, predicting, and designing ferroelectric domain structures and switching guided by the phase-field method. Annu Rev Mater Res. 2019;49(1):127–52. doi:10.1146/annurev-matsci-070218-121843.
118. Arlt G. Microstructure and domain effects in ferroelectric ceramics. Ferroelectrics. 1989;91(1):3–7. doi:10.1080/00150198908015725.
119. Zhuo F, Zhou X, Gao S, Höfling M, Dietrich F, Groszewicz PB, et al. Anisotropic dislocation-domain wall interactions in ferroelectrics. Nat Commun. 2022;13(1):6676. doi:10.1038/s41467-022-34304-7.
120. Höfling M, Zhou X, Riemer LM, Bruder E, Liu B, Zhou L, et al. Control of polarization in bulk ferroelectrics by mechanical dislocation imprint. Science. 2021;372(6545):961–64. doi:10.1126/science.abe3810.
121. Abdollahi A, Arias I. Phase-field modeling of fracture in ferroelectric materials. Arch Comput Methods Eng. 2015;22(2):153–81. doi:10.1007/s11831-014-9118-8.
122. Wilson ZA, Borden MJ, Landis CM. A phase-field model for fracture in piezoelectric ceramics. Int J Fract. 2013;183(2):135–53. doi:10.1007/s10704-013-9881-9.
123. Sridhar A, Keip M-A. A phase-field model for anisotropic brittle fracturing of piezoelectric ceramics. Int J Fract. 2019;220(2):221–42. doi:10.1007/s10704-019-00391-9.
124. Shet T, Bhimireddi R, Varma KBR. Grain size-dependent dielectric, piezoelectric and ferroelectric properties of sr2bi4ti5o18 ceramics. J Mater Sci. 2016;51(20):9253–66. doi:10.1007/s10853-016-0172-5.
125. Sharma VK, Nathawat R, Rathore SS. Dielectric properties correlation with microstructure in $ABi_4Ti_4O_{15}$ (A = Sr, Ba) bismuth layered ferroelectrics. Mater Adv. 2022;3(12):4890–8. doi:10.1039/d2ma00333c.
126. Bobić J, Ilić N, Veerapandiyan V, Petrović MV, Deluca M, Dzunuzović A, et al. Tailoring the ferroelectric and magnetic properties of $Bi_5Ti_3FeO_{15}$ ceramics by doping with Co and Y. Solid State Sci. 2022;123(2):106802. doi:10.1016/j.solidstatesciences.2021.106802.
127. Kinoshita K, Yamaji A. Grain-size effects on dielectric properties in barium titanate ceramics. J Appl Phys. 1976;47(1):371–3. doi:10.1063/1.322330.
128. Li C, Li J. Phase field study of ferroelastic domain switching behavior related to grain size in polycrystalline tetragonal zirconia. J Am Ceram Soc. 2025;108(7):e20495. doi:10.1111/jace.20495.
129. Lugovy M, Orlovskaya N, Neumann M, Aneziris CG, Jelitto H, Schneider GA, et al. Room temperature R-curve and stable crack growth behaviour of ZrB_2–SiC ceramic composites. Adv Appl Ceram. 2019;118(4):169–82. doi:10.1080/17436753.2018.1471443.
130. Wang M, Xia T, Geng LD. Phase-field study of crystallographic texturing in piezoelectric polycrystals. J Adv Dielectr. 2022;4(12):2244002. doi:10.1142/s2010135x22440027.

131. Abdollah A. Phase-field modeling of fracture in ferroelectric materials. [Ph. D. Thesis]. Spain: Universitat Politècnica de Catalunya; 2012.
132. Tan Y, Peng F, Li P, Liu C, Zhao J, Li X. A phase-field fracture model for piezoelectrics in hydrogen-rich environment. Int J Mech Sci. 2025;291(5):110092. doi:10.1016/j.ijmecsci.2025.110092.
133. Zhang M-H, Zhao C, Yan X, Wang S, Li S, Zheng Z, et al. Understanding the grain size dependence of functionalities in lead-free (Ba,Ca)(Zr,Ti)O_3. Acta Mater. 2024;276:120112. doi:10.1016/j.actamat.2024.120112.
134. Cotterill RMJ, Leffers T, Lilholt H. A molecular dynamics approach to grain boundary structure and migration. Philos Mag. 1974;30(2):265–75. doi:10.1080/14786439808206553.
135. Srolovitz DJ. Grain growth phenomena in films: a monte carlo approach. J Vac Sci Technol A Vac Surf Film. 1986;4(6):2925–31.
136. Cahn JW, Hilliard JE. Free energy of a nonuniform system. I. interfacial free energy. J Chem Phys. 1958;28(2):258–67. doi:10.1063/1.1744102.
137. Chen L-Q, Yang W. Computer simulation of the domain dynamics of a quenched system with a large number of nonconserved order parameters: the grain-growth kinetics. Phys Rev B. 1994;50(21):15752. doi:10.1103/physrevb.50.15752.
138. Moelans N, Blanpain B, Wollants P. Quantitative analysis of grain boundary properties in a generalized phase field model for grain growth in anisotropic systems. Phys Rev B Condens Matter Mater Phys. 2008;78(2):024113. doi:10.1103/physrevb.78.024113.
139. Ghiglione F, Ask A, Ammar K, Appolaire B, Forest S. Cosserat-phase-field modeling of grain nucleation in plastically deformed single crystals. J Mech Phys Solids. 2024;187(5):105628. doi:10.1016/j.jmps.2024.105628.
140. Zhang Y, Liu L. Grain growth behavior of ferroelectric ceramics under anisotropic grain boundary energy conditions simulated by the phase field method. Ceram Int. 2022;48(16):23767–76. doi:10.1016/j.ceramint.2022.05.030.
141. Chockalingam K, Dörfler W. Implementation of the coupled two-mode phase field crystal model with cahn-hilliard for phase-separation in battery electrode particles. Int J Numer Methods Eng. 2021;122(10):2566–80. doi:10.1002/nme.6632.
142. Gao X, Zhang Y, Liew KM. Electro-chemo-thermo-mechanical phase-field model for lithium penetration in solid electrolytes. Int J Mech Sci. 2025;307:110913. doi:10.1016/j.ijmecsci.2025.110913.
143. Sugathan S, Thekkepat K, Bandyopadhyay S, Kim J, Cha PR. A phase field model combined with a genetic algorithm for polycrystalline hafnium zirconium oxide ferroelectrics. Nanoscale. 2022;14(40):14997–5009. doi:10.1039/d2nr02678c.
144. Emdadi A, Zaeem MA. Phase-field modeling of crack propagation in polycrystalline materials. Comput Mater Sci. 2021;186(20–22):110057. doi:10.1016/j.commatsci.2020.110057.
145. Abdollahi A, Arias I. Numerical simulation of intergranular and transgranular crack propagation in ferroelectric polycrystals. Int J Fract. 2012;174(1):3–15. doi:10.1007/s10704-011-9664-0.
146. Lou XJ. Polarization fatigue in ferroelectric thin films and related materials. J Appl Phys. 2009;105(2):024101. doi:10.1063/1.3056603.
147. Damjanovic D. Ferroelectric, dielectric and piezoelectric properties of ferroelectric thin films and ceramics. Rep Prog Phys. 1998;61(9):1267. doi:10.1088/0034-4885/61/9/002.
148. Fang D, Jiang Y, Li S, Sun CT. Interactions between domain switching and crack propagation in poled $BaTiO_3$ single crystal under mechanical loading. Acta Mater. 2007;55(17):5758–67. doi:10.1016/j.actamat.2007.06.024.
149. Li YW, Li FX. *In situ* observation of electric field induced crack propagation in $BaTiO_3$ crystals along the field direction. Scr Mater. 2012;67(6):601–4. doi:10.1016/j.scriptamat.2012.06.020.
150. Matthias B, Von Hippel A. Domain structure and dielectric response of barium titanate single crystals. Phys Rev. 1948;73(11):1378. doi:10.1103/physrev.73.1378.
151. Forsbergh PW Jr. Domain structures and phase transitions in barium titanate. Phys Rev. 1949;76(8):1187. doi:10.1103/physrev.76.1187.
152. Nakamura T. Kinematic theory of ferroelectric domain growth. J Phys Soc Jpn. 1960;15(8):1379–86. doi:10.1143/jpsj.15.1379.

153. Floquet N, Valot CM, Mesnier MT, Niepce JC, Normand L, Thorel A, et al. Ferroelectric domain walls in $BaTiO_3$: fingerprints in XRPD diagrams and quantitative HRTEM image analysis. J De Phys III. 1997;7(6):1105–28.
154. Janovec V. Group analysis of domains and domain pairs. Czechoslov J Phys B. 1972;22(10):974–94. doi:10.1007/bf01690203.
155. Streiffer SK, Parker CB, Romanov AE, Lefevre MJ, Zhao L, Speck JS, et al. Domain patterns in epitaxial rhombohedral ferroelectric films. I. Geometry and experiments. J Appl Phys. 1998;83(5):2742–53. doi:10.1063/1.366632.
156. Li C, Xu X, Yang J, Liu Y, Sun L, Huang Z, et al. Domain engineering in ferroelectric nematics for nonlinear optical modulation. Sci Adv. 2025;11(28):eadu7362. doi:10.1126/sciadv.adu7362.
157. Zahn M, Müller AM, Kelley KP, Neumayer S, Kalinin SV, Kézsmarki I, et al. Reversible long-range domain wall motion in an improper ferroelectric. Nat Commun. 2025;16(1):1781. doi:10.1038/s41467-025-57062-8.
158. Liu S, Grinberg I, Rappe AM. Intrinsic ferroelectric switching from first principles. Nature. 2016;534(7607):360–3. doi:10.1038/nature18286.
159. Shin Y-H, Grinberg I, Chen IW, Rappe AM. Nucleation and growth mechanism of ferroelectric domain-wall motion. Nature. 2007;449(7164):881–4. doi:10.1038/nature06165.
160. Hu H-L, Chen L-Q. Three-dimensional computer simulation of ferroelectric domain formation. J Am Ceram Soc. 1998;81(3):492–500. doi:10.1111/j.1151-2916.1998.tb02367.x.
161. Ahluwalia R, Cao W. Computer simulations of domain pattern formation in ferroelectrics. In: AIP Conference Proceedings. College Park, MD, USA: American Institute of Physics; 2001. Vol. 582, p. 185–90.
162. Chen LQ, Shen J. Applications of semi-implicit fourier-spectral method to phase field equations. Comput Phys Commun. 1998;108(2–3):147–58. doi:10.1016/s0010-4655(97)00115-x.
163. Li YL, Hu SY, Liu ZK, Chen LQ. Effect of substrate constraint on the stability and evolution of ferroelectric domain structures in thin films. Acta Mater. 2002;50(2):395–411. doi:10.1016/s1359-6454(01)00360-3.
164. Li Y, Cheng X, Zhu D, Gan Z. Influence of domain switching process on the electrical fatigue behavior of ferroelectrics. Ceram Int. 2020;46(15):24213–24. doi:10.1016/j.ceramint.2020.06.201.
165. Wang J, Zhang T. Phase field simulations of polarization switching-induced toughening in ferroelectric ceramics. Acta Mater. 2007;55(7):2465–77. doi:10.1016/j.actamat.2006.11.041.
166. Kim Q, Somoano R, Lowe Ma C, Coleman LB, Moopen A. Studies of defects in improper ferroelectrics. Ferroelectrics. 1981;36(1):435–8. doi:10.1080/00150198108218147.
167. Geng L, Yang W. Defect agglomeration in ferroelectric ceramics under cyclic electric field. Sci China Ser E Technol Sci. 2008;51(8):1296–305.
168. Brennan C. Model of ferroelectric fatigue due to defect/domain interactions. Ferroelectrics. 1993;150(1):199–208. doi:10.1080/00150199308008705.
169. Park CH, Chadi DJ. Microscopic study of oxygen-vacancy defects in ferroelectric perovskites. Phys Rev B. 1998;57(22):R13961. doi:10.1103/physrevb.57.r13961.
170. Liu B, Fang D, Hwang K. Electric-field-induced fatigue crack growth in ferroelectric ceramics. Mater Lett. 2002;54(5–6):442–6. doi:10.1016/s0167-577x(01)00607-3.
171. Soh AK, Fang D-N, Lee K-L. Fracture analysis of piezoelectric materials with defects using energy density theory. Int J Solids Struct. 2001;38(46–47):8331–44. doi:10.1016/s0020-7683(01)00080-4.
172. Geng L, Yang W. Agglomeration of point defects in ferroelectric ceramics under cyclic electric field. Model Simul Mater Sci Eng. 2006;14(2):137. doi:10.1088/0965-0393/14/2/002.
173. Geng L, Yang W. Coalescence of pore columns by domain switching. Acta Mech Sin. 2006;22(3):207–16. doi:10.1007/s10409-006-0003-z.
174. Mohanty S, Kumbhar PY, Swaminathan N, Annabattula R. A phase-field model for crack growth in electro-mechanically coupled functionally graded piezo ceramics. Smart Mater Struct. 2020;29(4):045005. doi:10.1088/1361-665x/ab7145.
175. Suo Z. Models for breakdown-resistant dielectric and ferroelectric ceramics. J Mech Phys Solids. 1993;41(7):1155–76. doi:10.1016/0022-5096(93)90088-w.

176. Scott JF, Azuma M, de Araujo CAP, McMillan LD, Scott MC, Roberts T. Dielectric breakdown in high-ε films for ULSI drams: II. barium-strontium titanate ceramics. Integr Ferroelectr. 1994;4(1):61–84. doi:10.1080/10584589408018661.
177. Stolichnov I, Tagantsev A, Setter N, Okhonin S, Fazan P, Cross JS, et al. Dielectric breakdown in (Pb,La)(Zr,Ti)O_3 ferroelectric thin films with pt and oxide electrodes. J Appl Phys. 2000;87(4):1925–31. doi:10.1063/1.372114.
178. Shkuratov SI, Baird J, Talantsev EF. Extension of thickness-dependent dielectric breakdown law on adiabatically compressed ferroelectric materials. Appl Phys Lett. 2013;102(5):052906. doi:10.1063/1.4791597.
179. Cain MG. Dielectric breakdown in dielectrics and ferroelectric ceramics. In: Characterisation of ferroelectric bulk materials and thin films. Berlin/Heidelberg, Germany: Springer; 2014. p. 243–66.
180. Nguyen MD, Nguyen CTQ, Vu HN, Rijnders G. Experimental evidence of breakdown strength and its effect on energy-storage performance in normal and relaxor ferroelectric films. Curr Appl Phys. 2019;19(9):1040–5. doi:10.1016/j.cap.2019.06.005.
181. Wu Z, Peng Y, Guo Q, Zhou H, Gong L, Liu Z, et al. Multilayer heterogeneous dielectric films with simultaneously improved dielectric constant and breakdown strength. Mater Today Commun. 2022;32:103857. doi:10.1016/j.mtcomm.2022.103857.
182. Mi Z, Zhang Y, Hou X, Wang J. Phase field modeling of dielectric breakdown of ferroelectric polymers subjected to mechanical and electrical loadings. Int J Solids Struct. 2021;217(7):123–33. doi:10.1016/j.ijsolstr.2021.02.009.
183. Cai Z, Zhu C, Wang X, Li L. Phase-field modeling of the coupled domain structure and dielectric breakdown evolution in a ferroelectric single crystal. Phys Chem Chem Phys. 2019;21(29):16207–12. doi:10.1039/c9cp02860a.
184. Cai Z, Feng P, Zhu C, Wang X. Dielectric breakdown behavior of ferroelectric ceramics: the role of pores. J Eur Ceram Soc. 2021;41(4):2533–8. doi:10.1016/j.jeurceramsoc.2020.11.051.
185. Khondabi M, Ahmadvand H, Javanbakht M. Revisiting the dielectric breakdown in a polycrystalline ferroelectric: a phase-field simulation study. Adv Theory Simul. 2023;6(1):2200314. doi:10.1002/adts.202200314.
186. Shen ZH, Wang JJ, Jiang JY, Huang SX, Lin YH, Nan CW, et al. Phase-field modeling and machine learning of electric-thermal-mechanical breakdown of polymer-based dielectrics. Nat Commun. 2019;10(1):1843. doi:10.1038/s41467-019-09874-8.
187. Schreiber C, Müller R, Kuhn C. Phase field modeling of fatigue crack initiation and growth under various loading situations. Proc Appl Math Mech. 2021;20(1):e202000029. doi:10.1002/pamm.202000029.
188. Zhu T, Fang F, Yang W. Fatigue crack growth in ferroelectric ceramics below the coercive field. J Mater Sci Lett. 1999;18(13):1025–7. doi:10.1023/a:1006663108103.
189. Fang D, Liu B, Sun CT. Fatigue crack growth in ferroelectric ceramics driven by alternating electric fields. J Am Ceram Soc. 2004;87(5):840–6. doi:10.1111/j.1551-2916.2004.00840.x.
190. Fang F, Yang W, Zhang FC, Luo HS. Fatigue crack growth for $BaTiO_3$ ferroelectric single crystals under cyclic electric loading. J Am Ceram Soc. 2005;88(9):2491–7. doi:10.1111/j.1551-2916.2005.00436.x.
191. Salz CRJ, Hoffman M, Westram I, Rödel J. Cyclic fatigue crack growth in PZT under mechanical loading. J Am Ceram Soc. 2005;88(5):1331–3. doi:10.1111/j.1551-2916.2005.00235.x.
192. Westram I, Ricoeur A, Emrich A, Rödel J, Kuna M. Fatigue crack growth law for ferroelectrics under cyclic electrical and combined electromechanical loading. J Eur Ceram Soc. 2007;27(6):2485–94. doi:10.1016/j.jeurceramsoc.2006.09.010.
193. Wang BL, Han JC. An accumulation damage model for fatigue fracture of ferroelectric ceramics. Eng Fract Mech. 2007;74(9):1456–67.
194. Glaum J, Hoffman M. Electric fatigue of lead-free piezoelectric materials. J Am Ceram Soc. 2014;97(3):665–80. doi:10.1111/jace.12811.
195. Genenko YA, Glaum J, Hoffmann MJ, Albe K. Mechanisms of aging and fatigue in ferroelectrics. Mater Sci Eng B. 2015;192:52–82. doi:10.1016/j.mseb.2014.10.003.
196. Lange S, Ricoeur A. High cycle fatigue damage and life time prediction for tetragonal ferroelectrics under electromechanical loading. Int J Solids Struct. 2016;80:181–92. doi:10.1016/j.ijsolstr.2015.11.003.
197. Kozinov S, Kuna M. Simulation of fatigue damage in ferroelectric polycrystals under mechanical/electrical loading. J Mech Phys Solids. 2018;116(2):150–70. doi:10.1016/j.jmps.2018.03.013.

198. Li Y, Chen Z, Duan G. Fatigue crack growth mechanism in ferroelectric ceramics under alternating electric field: an investigation by digital image correlation technique. Acta Mater. 2022;235(7):118065. doi:10.1016/j.actamat.2022.118065.
199. Xie Q, Qi H, Li S, Yang X, Shi D. A phase-field model for mixed-mode elastoplastic fatigue crack. Eng Fract Mech. 2023;282:109176. doi:10.1016/j.engfracmech.2023.109176.
200. Waseem S, Erdogan C, Yalçinkaya T. Phase field modeling of fatigue crack growth retardation under single cycle overloads. Int J Fatigue. 2024;179:108064. doi:10.1016/j.ijfatigue.2023.108064.
201. Tang W, Yi M, Chen L-Q, Guo W. Classical fatigue theory informed phase-field model for high-cycle fatigue life and fatigue crack growth. Eng Fract Mech. 2024;306(6):110212. doi:10.2139/ssrn.4800112.
202. Alhada-Lahbabi K, Deleruyelle D, Gautier B. Machine learning surrogate for 3D phase-field modeling of ferroelectric tip-induced electrical switching. npj Comput Mater. 2024;10(1):197. doi:10.1038/s41524-024-01375-7.
203. de Moraes EAB, Salehi H, Zayernouri M. Data-driven failure prediction in brittle materials: a phase field-based machine learning framework. J Mach Learn Model Comput. 2021;2(1):65–89.
204. Shang L, Zheng S, Wang J, Wang J. Physics-informed neural networks incorporating energy dissipation for the phase-field model of ferroelectric microstructure evolution. arXiv:2409.02959. 2024.
205. Konale A, Srivastava V. A physics-informed neural network for modeling fracture without gradient damage: formulation, application, and assessment. J Mech Phys Solids. 2025;206(7):106395. doi:10.1016/j.jmps.2025.106395.